Vaccination and immigration rates influence raccoon rabies elimination and recolonization in simulated urban-suburban landscapes

Emily M. Beasley[1] and Timothée Poisot[1]

[1]Département de Sciences Biologiques, Université de Montréal, Montréal, Québec, Canada

Correspondence: Emily M. Beasley, beasley.em@gmail.com

Abstract

The raccoon variant of the rabies virus (RRV) is primarily managed in the eastern United States and Canada via distribution of oral rabies vaccine (ORV) baits. The goal of ORV distribution is to reach seroprevalence rates (an index of population immunity) of 60%, the threshold thought to eliminate RRV. Seroprevalence rates in urban areas rarely reach target levels, predictably leading to rabies outbreaks. However, many managed urban areas have spent several years rabies-free, suggesting RRV can be eliminated from urban areas at below-target seroprevalence rates. Using an agent-based model to simulate raccoon populations in urban landscapes, we examined 1) effects of varying vaccination and immigration rates on rabies elimination probability and time to elimination, and 2) what vaccination threshold, if any, prevents subsequent rabies recolonization events. Rabies elimination rates ranged from 52–98% with a median of 82.6%. Vaccination rates increased elimination probability (1.6% per 10% increase in vaccination) and time to elimination (11 weeks per 10% increase in vaccination), whereas the weekly immigration rate and immigrant prevalence rate reduced elimination probability (3.7% per additional expected weekly immigrant and 1.1% per 1% increase in rabies prevalence, respectively). Recolonization was common and highly stochastic, with a recolonization probability ranging from 12.5–100% with a median of 89.5%. Immigration rates and immigrant prevalence increased the weekly probability of recolonization after rabies was eliminated (0.6% per additional expected weekly immigrant and 1.6% per 1% increase in rabies prevalence, respectively). Vaccination decreased weekly recolonization probability (1.6% per 10% increase in vaccination rate)

and reduced the number of rabies cases following a recolonization event. Based on these results, we recommend continuous vaccination within the urban area and along raccoon movement corridors to prevent infected individuals from entering rabies-free areas, as both vaccination and immigration variables affected the likelihood of recolonization. Understanding long-distance movements of host individuals is crucial for managing diseases such as rabies which likely persist at the regional scale.

Keywords: raccoon rabies, urban ecology, immigration, rabies management, agent-based models, landscape ecology

Introduction

Lyssavirus rabies remains a zoonosis of global concern for both wildlife and humans (Elmore et al., 2017; Rupprecht et al., 2002; Vercauteren et al., 2012). Transmitted primarily through direct contact with an infected individual, rabies is nearly always fatal once observable symptoms appear (Rupprecht et al., 2002). Because the primary mode of transmission is host-to-host contact, understanding the movement ecology and social behavior of a given host species is essential for understanding rabies transmission. In the eastern United States and Canada, raccoons (*Procyon lotor*) are the primary reservoir of the raccoon variant of the rabies virus (RRV) and are the largest source of terrestrial wildlife cases (Elmore et al., 2017; Gilbert A, 2018). Due to their broad geographic range and high tolerance of human-altered habitats (Lotze & Anderson, 1979; Randa & Yunger, 2006; Slate et al., 2020), and wide variation in demography and behavior (Prange et al., 2004; Prange & Gehrt, 2004; Slate et al., 2020), understanding raccoon ecology as it relates to rabies dynamics is still an active area of management concern.

Since the 1990s, management of RRV has been largely successful in controlling the geographic spread of the virus due to a combination of enhanced surveillance and vaccination (Davis et al., 2021; Elmore et al., 2017; Kirby et al., 2017; Rosatte et al., 2009), especially distribution of oral rabies

vaccines (ORV). In rural areas, ORV deployment appears to achieve target seroprevalence rates (60%, Gilbert et al., 2018; Johnson et al., 2021) thought to be needed for RRV elimination (McClure et al., 2020; Rees et al., 2013; Reynolds et al., 2015). Despite the success of ORV campaigns in rural areas, management has proven challenging in urban and suburban landscapes, with seroprevalence rates typically below 40% (Beasley et al., 2024; Bigler et al., 2021; Mainguy et al., 2012). Urban-suburban raccoon populations often have very different demographics than their rural counterparts, including higher population densities, smaller home ranges, and differences in social behavior (Prange et al., 2003, 2004; Rosatte et al., 2010; Slate et al., 2020). Furthermore, urban habitats are often highly fragmented and can contain higher densities of nontarget bait competitors (e.g. virginia opossums *Didelphis virginiana*, coyotes *Canis latrans*), which may influence the rate at which raccoons encounter ORV baits (Beasley et al., 2024; Haley et al., 2019). These ecological characteristics likely influence disease dynamics in urban-suburban areas, such as by increasing the duration of epizootics (Recuenco et al., 2007). Compounding the ecological challenges are logistical difficulties in bait distribution, resulting in bait distribution that is often along roads rather than in preferred urban raccoon habitat (Beasley et al., 2024; Bigler et al., 2021).

As a result of these challenges, ORV is much less effective in urban and suburban habitats, leading to chronically suboptimal seroprevalence rates (Bastille-Rousseau et al., 2024). Managers have developed strategies to increase the effectiveness of ORV campaigns, such as targeting preferred raccoon habitat (McClure et al., 2022), the use of bait stations, and supplementing ORV distribution with trap-vaccinate-release (TVR) campaigns (Bastille-Rousseau et al., 2024). The use of TVR has proven effective in increasing seroprevalence rates in urban landscapes, and its use in addition to ORV has resulted in significant reductions in rabies cases in Hamilton, Ontario (Bastille-Rousseau et al., 2024).

Despite low seroprevalence rates in urban areas, some vaccination campaigns have been successful in reaching local elimination (e.g. Burlington, VT, USA 2017–2022, Beasley et al., 2024;

Ontario, Canada 2024, Ontario Ministry of Natural Resources and Forestry, 2025). The reasons for these successes are unclear. It is possible that seroprevalence rates lower than the current target of 60% are sufficient for elimination; particularly given the estimated effective reproduction number R_e is close to 1 (Biek et al., 2007). However, a recent raccoon rabies outbreak in Burlington, Vermont ongoing since 2023 (Vermont Department of Health, 2025) suggests that low vaccination rates may leave urban and suburban areas vulnerable to recolonization of the virus after elimination has been achieved.

Understanding the role of vaccination rates, immigration rates, and the interaction between them is therefore critical for assessing the vulnerability of urban areas to rabies recolonization after the virus has been eliminated. However, the relative paucity of raccoon movement data across the urban-rural gradient makes empirical assessments impossible. Agent-based models are a powerful tool for evaluating the effects of various factors on disease dynamics, as one can readily modify model parameters to explore their effects across a broad range of possible ecological conditions. Using a spatially explicit agent-based model applied to simulated landscapes, we explored the effect of vaccination and immigration on rabies elimination and recolonization under varying vaccination rates. More specifically, we examined how 1) vaccination rates, 2) immigration rates, 3) rabies prevalence of immigrants, and 4) frequency of immigration (continuous vs. seasonal) impacted the probability and timing of rabies elimination and subsequent recolonization. Based on previous work, we predict that rabies can be eliminated from landscapes with vaccination rates less than 60% (Acheson et al., 2023; Beasley et al., 2024), and increasing vaccination rates will reduce the time it takes to achieve elimination. We predict increasing rates of immigration will 1) increase the time to successfully reach elimination by augmenting the susceptible population of raccoons, and 2) increase the probability of rabies re-colonization by influencing invasion pressure.

Materials and Methods

Full modeling methodology following the Overview, Design Concepts, Details (ODD) protocol for describing individual-based models (Grimm et al., 2006, 2010) can be found in Appendix 1.

Landscape Creation

We modeled urban-suburban landscapes by constructing 60 x 60 rasters using the package NeutralLandscapes.jl, which is based on the Python package NLMPy, in Julia 1.9.2 (Bezanson et al., 2017; Etherington et al., 2015; Poisot et al., 2023). Each cell was 0.5 x 0.5 km for a total landscape size of 30 km^2, which is the approximate size of the greater Burlington, VT area. We created habitat clusters using the mid-point displacement algorithm (Fournier et al., 1982), which takes as input an autocorrelation parameter. We used the function `lsm_l_ai` in the R package landscapemetrics (Hesselbarth et al., 2019) to calculate autocorrelation from land cover data from the greater Burlington area (Homer et al., 2015). We re-classified the resulting raster into discrete habitats, the relative proportions of which were derived from the Burlington land cover data. To prevent boundary effects (Koen et al., 2010), a 5-cell buffer on each edge of the 60x60 raster was designated as a unique "buffer" habitat. We chose the greater Burlington area as our example urban-suburban landscape because it is the site of extensive empirical data for informing model parameters, and the site of an ongoing outbreak as of this writing. Yet, our model is generalizable enough to resemble similar cities near ORV zones such as Syracuse, NY and Sherbrooke, QC.

Raccoon movement and demographics

Raccoon movement in the simulated landscapes was governed using weighted probabilities. At each time step, a raccoon could move to any of its eight neighboring cells or stay in its current cell. The probability of selecting a given cell was weighted according to a habitat selection function, in which some habitats were more likely to be selected than others (McClure et al., 2022), a home range attractor, in which cells further from a raccoon's home cell were less likely to be selected as the

destination cell (McClure et al., 2022; Signer et al., 2017), and conspecific avoidance, in which individuals had a higher probability of selecting cells with fewer raccoons. The home range attractor was calculated as a weighted probability:

$$p\left(c_{t+1}\right) \propto \exp\left(-\omega\, d\left(c_{t+1}\right)\right) \qquad \text{(Eq. 1)}$$

In which $p(\boldsymbol{c}_{t+1})$ the probability of a raccoon occupying cell c within the raccoon's Moore neighborhood at time $t+1$, ω the strength of attraction towards the home range attractor, and $\boldsymbol{d}(\boldsymbol{c}_t)$ the squared distance between target cells and the home cell. The squared distance between cells was calculated by:

$$d\left(c_{t+1}\right) = \frac{r\left\{\left(x_t - x_h\right)^2 + \left(y_t - y_h\right)^2\right\}}{100} \qquad \text{(Eq. 2)}$$

In which (x_t, y_t) are x and y coordinates of target cell t, (x_h, y_h) are the x and y coordinates for the raccoon's home cell, and r is the resolution of each grid cell. Raccoons younger than the age of independence (20 weeks) always moved to the same cell as their mother (Viard et al., 2022). Raccoons could not move outside of the landscape boundaries unless they were dispersing (see below).

Raccoon demographics followed the literature where data is available (Appendix 2, Table 2). Female raccoons at least 52 weeks of age were eligible to reproduce, and the probability of reproduction in a given year was equal for all eligible raccoons. Births occurred in week 18 of each year of the simulation (aligning with previous work in the same biological system, e.g. Acheson et al., 2023), with the litter size drawn from a Poisson distribution with an expected value (λ) of four. All raccoons were subject to stochastic mortality, in which the probability of mortality in a given week was 0.1%. Old age mortality triggered at 416 weeks (eight years) of age. Density-related mortality, in which raccoons occupying cells with more than 30 raccoons experienced elevated mortality rates, varied depending on the age of the raccoon (Appendix 2, Table 2). Because raccoon movement includes conspecific avoidance, raccoons could move into a less crowded cell in the previous time step and avoid carrying capacity mortality unless adjacent cells were similarly over-occupied. Raccoons

younger than the age of independence were killed and removed from the simulation if their mother was dead.

Raccoons less than 52 weeks of age dispersed every year between weeks 41–45 of the simulation. For each dispersing raccoon, the direction of movement was determined by randomly selecting one of eight directions of movement corresponding to the 8 neighboring cells (Cullingham et al., 2008). The raccoon moved in that direction for a distance drawn from a Poisson distribution with an expected value (λ) of 0.75 cells: thus, it was possible for an agent to have a dispersal distance of 0 and remain in place. The dispersal function was repeated four times, one for each week of the dispersal period; each raccoon therefore dispersed an expected distance of 3 cells (1.5 km, Rees et al., 2008). Raccoons over 1 year of age could also disperse, but only dispersed if they occupied a cell above carrying capacity, and traveled a smaller expected dispersal distance ($\lambda = 2$ cells or 1 km, Rees et al., 2008). Although there are slight differences in dispersal distances between male and female raccoons (Rees et al., 2008), at this grain size the difference is negligible. Raccoons that left the landscape were removed from the simulation.

We simulated two types of raccoon immigration in which individuals entered the landscape from outside the simulated population: “consistent” immigration in which the landscape received a steady stream of a few immigrants per week, and “seasonal” immigration in which the landscape received a much larger number of weekly immigrants in a specific time frame. In landscapes with consistent immigration, the number of weekly immigrants was drawn from a Poisson distribution with an expected value (λ) taking values ranging from 0.5–2.5 at intervals of 0.5. These values correspond to numbers of immigrants that are less than 1% of the resident population. Landscapes with seasonal immigration had a weekly immigration rate drawn from a Poisson distribution with an expected value of $\lambda*5$, but immigration only occurred in weeks 40–50 to coincide with the annual dispersal period. In both cases, landscapes received approximately equal numbers of immigrants over the course of the simulation period. Immigrants were equally likely to be male or female and ranged from 1–8 years of

age. When entering the landscape, immigrants were randomly assigned a starting location, direction of movement, and a movement distance, the latter drawn from a Poisson distribution with an expected movement value (λ) of 10 cells. Immigration occurred uniformly across landscape boundaries. Movement directions that would immediately take the agent outside of the landscape boundaries were excluded; all other movement directions were equiprobable. Immigrants had a 10% probability of being immune to rabies when they entered the simulation, matching natural levels of rabies antibodies (Slate et al., 2014). Although it is likely that some raccoons immigrate from an ORV management zone and would have vaccine-induced rabies immunity, the proportion of total immigrants represented by these individuals likely varies from city to city, and we assumed baseline susceptibility to model a worst-case scenario. Immigrants were randomly assigned an infected state as the outcome of a Bernoulli trial with varying probabilities of success, ranging from 0–0.06 at intervals of 0.015. These rates fall within the range of previously documented disease incidence rates (Jenkins et al., 1988; Ma et al., 2021; Roscoe et al., 1998). Furthermore, there is evidence that infected individuals move further than non-infected individuals (Rosatte et al., 2006; Roscoe et al., 1998), therefore long-distance immigrants could have higher infection rates than residents.

Disease dynamics

We modeled the disease as a spatially explicit SEIR model with additional demographic processes (Fig. 1). The spatially explicit component of the model affects the force of infection parameter λ, or the probability of infectious raccoon infecting a susceptible raccoon, which varies based on the proximity of each raccoon in a given week. Infectious raccoons were assumed to be more likely to infect raccoons that were located within 0.5 km of the infectious raccoon's current position (core home range transmission, $\lambda_1 = 0.02$) due to a high degree of overlap in weekly home ranges, and therefore a higher probability of contact (Habib et al., 2011; Van der Wal et al., 2014, but see Yang et al., 2023). Susceptible raccoons between 0.5 and 1 km of the infected raccoon were less likely to be

infected compared to individuals in the same cell as an infected raccoon ($\lambda_2 = 0.006$) due to a lower degree of home range overlap. Raccoons occupying a cell more than 1 km from the infected individual could not be infected by that individual due to small home ranges of urban raccoons.

After a susceptible raccoon entered the exposed state, it could potentially recover from the disease and acquire permanent immunity with a weekly probability of 0.002, which corresponded to an 8–12% probability of recovery over the duration of the disease (Slate et al., 2014). Raccoons which did not recover in a given week could transition to the infectious state with a probability $\delta \sim Beta(t, 5)$, in which *t* is the number of weeks the raccoon has spent in the exposed state. This results in a transition probability that increases over time for a typical incubation period of 4–6 weeks (Tinline et al., 2002). Raccoons in the infectious state always died after being infectious for 1 week (Hanlon et al., 2007).

Most agents transitioned to the recovered state via vaccination. Vaccination occurred during week 35 of the simulation, and the probability of vaccination was based on the agent's age and location. Agents in the buffer which were at least 52 weeks old had a vaccination probability of 60% (Fehlner-Gardiner et al., 2012). Agents elsewhere in the landscape that were at least 1 year old were vaccinated with a user-defined probability that ranged from 0–80% at 10% intervals. Agents less than 1 year old had a vaccination probability that was half of the probability for agents older than 1 year (Beasley et al., 2024). Once a raccoon entered the recovered state, it permanently remained in that state.

Model specifications.

Raccoon populations were initialized with a mean population density of 6/km^2. Initial ages of the raccoons were randomly assigned from a range of 52–416 weeks (1–8 years). Raccoons were randomly assigned an initial vaccination status as the outcome of a Bernoulli trial with a probability of success that varied based on the adult vaccination rate defined at the start of the simulation. The buffer

zone of the simulation area was then populated at a density of 4/km^2 with a vaccination rate of 60%, with ages of the raccoons as described above.

Rabies was introduced at the beginning of year two of the simulation to allow the raccoon population dynamics to stabilize. In each simulation, 10 susceptible raccoons (see *Parameter Sensitivity Analysis* below) were randomly selected from the population to enter the exposed state. Disease dynamics then proceeded as described above.

Simulation replicates varied in adult vaccination rate, immigration type, immigration rate, and the proportion of immigrants that were infected (Appendix 2, Table 2). We ran 50 replicates for each combination of parameters; each simulation ran for 11 years (one year to stabilize population + 10 years after rabies introduction). Data visualization was completed in R version 4.1.2 (R Core Team, 2021); R_0 was calculated using the maximum likelihood (White et al., 2009) and R_e was calculated using the sequential Bayesian method (Bettencourt & Ribeiro, 2008) in the R package `R0` (Boelle & Obadia, 2023). We compared 1) the probability of rabies elimination, 2) length of the initial outbreak, 3) weekly probability of recolonization, and 4) cases after recolonization across the four variables. We defined a recolonization event as a period in which, after rabies was completely eliminated from the landscape, infected individuals were present in the landscape for a duration of at least 10, 26, and 52 consecutive weeks. We chose a minimum 10-week duration because, based on the latent period of the disease (Fig. 2-3), we can assume with near certainty that the disease was transmitted to at least one other individual. We compared weekly probability of recolonization rather than total probability because simulations in which elimination was achieved more rapidly had a longer time period in which rabies could potentially recolonize.

Parameter Sensitivity Analysis

We performed parameter sensitivity analyses to evaluate the effects of carrying capacity mortality rates, rabies transmission rates, the number of starting cases, and landscape size on metrics

such as population density, elimination probability, and effective reproduction number R_e. We chose these parameters for sensitivity analyses because they are either difficult to measure empirically and/or can have a large impact on simulation outcomes. A full description of the parameter sensitivity analyses can be found in Appendix 2.

We tested various cell-level carrying capacity (K_{max}) and carrying capacity-associated mortality rates to select values which yielded population densities that were comparable to those in Burlington (15 raccoons per km^2 in summer and 11 per km^2 in fall). Carrying capacity mortality was applied to cells containing greater than K_{max} individuals. Carrying capacity mortality also varied based on raccoon age. We selected a K_{max} of 30, a mortality rate of 0.0075 for raccoons at least 52 weeks old, and a mortality rate of 0.015 for raccoons less than 52 weeks old because this combination 1) yielded population densities comparable to those in Burlington, 2) resulted in populations that were steadily growing, and 3) yielded a less variable population size compared to other parameter combinations that met conditions 1 and 2 (Figs. 2-4, 2-5).

We tested several combinations of values of core home range (λ_1, corresponding to the transmission rate to raccoons within 0.5 km of the infectious raccoon) and peripheral home range (λ_2, corresponding to transmission to raccoons 0.5–1 km of the infectious agent) transmission rates. We first tuned the core home range transmission rate by simulating a wide sweep of values between 0.001 and 0.5 on a logarithmic scale (McClure et al., 2020). From these, we selected promising transmission rates based on 1) rabies persistence in at least 1 complete simulation, 2) median duration of rabies persistence, 3) median weekly symptomatic cases, and 4) a mean effective reproduction number R_e close to the empirical value of 1.13. Transmission rates of 0.0224 and 0.0349 met these criteria. We then tested a values for transmission rates at the periphery of an infected agent's weekly home range λ_2. We began with a logarithmic sequence of values ranging from 0.001–0.03 with λ_1 fixed at 0.0275 (approximate midpoint between the selected λ_1 values). We evaluated λ_2 values using the same criteria.

Based on the results of the broad sweep of λ values, we chose to further test λ_1 values from 0.01–0.03 at intervals of 0.5, and λ_2 values of 0.004–0.007 at intervals of 0.001. We ultimately chose a λ_1 of 0.02 and a λ_2 of 0.006 based on the criteria listed above (Figs. 2-12 – 2-15).

We tested the effects of the number of starting cases on rabies elimination probability and time, median and maximum weekly cases, and the effective reproductive rate R_e. We completed simulations with 5, 10, 20, and 40 starting cases, with 20 replicates each and transmission rates as above. The number of starting cases had no clear effect on elimination probability, median weekly cases, time to elimination, or R_e (Figs. 2-16 – 2-18). The number of starting cases had a clear effect on maximum weekly cases: simulations with 20 and 40 starting cases had an observably higher maximum than simulations with 5 or 10 starting cases (Fig. 2-19); we therefore chose 10 starting cases per simulation.

To examine our ability to generalize our results, we tested the effect of landscape size on rabies elimination and median prevalence by simulating 20 replicates each of landscapes with a 40x40, 60x60, 80x80, and 100x100 cell grid. Elimination probability decreased with landscape size: elimination was reached in 80% of 40x40 landscapes, 65% of 60x60 landscapes, and 5% of the largest landscape sizes. Rabies prevalence did not differ between simulations with different landscape sizes (Fig. 2-22).

Results

Rabies was eliminated at least once in 82.6% of simulated landscapes, with an estimated R_0 of 1.39 (interquartile range 1.04–1.58). The estimated value of R_e varied based on vaccination rates (Fig. 3-1) but was typically 1.17 in simulations where the adult vaccination rate was 0%. Rabies prevalence varied between simulations and fluctuated seasonally within each simulation, but typically ranged from 0–0.004 (95% CI) with a maximum prevalence of 0.012 (Fig. 3-2).

Elimination probability ranged from 52–98% and was strongly influenced by vaccination rates, weekly immigration rates, and immigrant disease rates (Fig. 2). Elimination probability increased with vaccination rates: for every increase in vaccination rates by 10%, elimination probability increased by

1.59%, although this varied based on immigration variables (Fig. 2). Increasing immigration by 1 expected immigrant per week reduced elimination probability by approximately 3.7% (Fig. 2A) and increasing the immigrant disease rate by 1% decreased elimination probability by approximately 1.1% (Fig. 2B). Immigration type did not have a clear effect on elimination rates.

For simulations in which elimination was reached, each 10% increase in vaccination decreased time to elimination by approximately 11 weeks (Fig. 3). For every 1% increase in the disease rate of immigrants, time to elimination increased by 1.34 weeks. Neither immigration rate nor immigration type had a clear effect on time to elimination.

Qualitative effects of vaccination and immigration variables were consistent regardless of how recolonization was defined; however, effects were most clear when a novel outbreak lasted at least 26 weeks (6 months). Recolonization probability ranged from 12.5–100% (95% CI), with a median of 89.5%; weekly recolonization probability ranged from 0.289–12.5% (95% CI) with a median of 0.885%. Expected weekly immigrants, the disease rate of immigrants, and vaccination rates influenced weekly recolonization probability, although the effects of these variables were relatively small (Fig. 4). Increasing immigration rates by 1 expected immigrant per week increased weekly colonization probability by 0.6% and increasing immigrant prevalence by 1% increased weekly colonization probability by 0.16% (Fig. 4a). Increasing vaccination rates by 10% reduced weekly colonization probability by 0.16%, predominately by reducing unusually high colonization probabilities (Fig. 4c). Results in which a “recolonization” was defined as 10 weeks and 52 weeks can be found in Appendix 3.

There were no clear effects of any variables on the duration of recolonization events. When immigration was continuous, recolonization events lasted slightly longer when they began between the birth pulse and juvenile independence, but there was a high degree of overlap between developmental time periods (Appendix 3, Fig. 5). The number of cases after the initial elimination increased with expected weekly immigrants (~155 cases per increase by 1 weekly immigrant) and immigrant

prevalence (~59 per 1% increase in prevalence) and decreased with vaccination rates (~25 cases per 10% increase in vaccination rates, Appendix 3, Fig. 7).

Discussion

In line with our predictions, rabies elimination was possible at vaccination rates less than the target rate of 60%: in fact, elimination was common, occurring in more than 80% of simulations. The probability and speed of rabies elimination increased with increasing vaccination rates; whereas increased immigration rates resulted in lower probabilities of rabies elimination. Rabies elimination was facilitated by the relatively small extent of the simulated landscape and small raccoon home range sizes, as disease mortality and (when applicable) vaccination sufficiently reduced localized densities of susceptible individuals to reduce R_e below 1. Additionally, all immigration variables influenced rabies recolonization in a manner consistent with our predictions: higher immigration rates and higher disease prevalence in immigrants increased the likelihood of recolonization. Vaccination decreased recolonization rates and reduced the number of cases associated with recolonization events.

Our model, like all agent-based models, represents a simplified version of reality, the assumptions of which may impact the results. Modeling decisions such as the grain size of the simulated landscapes and the use of a step function to model disease transmission could have influenced the results (see Appendices 1–2 for details on modeling decisions and rationale). It is possible that these decisions resulted in simulated enzootic periods that are shorter than empirical county-level enzootic periods (Childs et al., 2000), but our short enzootic periods could also be an artifact of the small landscape extent. Given that our estimated R_e at vaccination rates of 0% is consistent with previous estimates of raccoon rabies R_e *(Biek et al., 2007)* and our estimated R_0 is consistent with estimates of R_0 among other rabies reservoirs (Hampson et al., 2009; Townsend et al., 2013; but see Li et al., 2024), our simulations are a sufficiently reasonable approximation of reality to produce useful results.

Our approach complements previous agent-based models for examining rabies transmission and management strategies by providing a generalizable framework that still captures the fine-scale processes impacting rabies transmission in urban-suburban landscapes. Agent-based models such as the Ontario Rabies Model (Acheson et al., 2023; Bastille-Rousseau et al., 2024; Rees et al., 2013; Tinline et al., 2007) and others (e.g. McClure et al., 2020) are powerful tools for assessing rabies transmission at broad spatial extents, but the large grain size of these models fails to capture the small-scale raccoon movement ecology driving transmission in urban areas. McClure et al. (2022) successfully captured urban raccoon movements and assessed their impacts on ORV effectiveness. If used to model rabies transmission, the smaller grain size and time step would likely outperform our model, albeit with a large trade-off in computation time. Agent-based models remain promising tools for informing rabies management strategies; however, it is essential to select the appropriate model for the spatial scale and research question of interest.

Our results suggest that, while vaccination rates at or above target levels offer some protection against recolonization events, they are not sufficient to prevent recolonization entirely. This may be due to high raccoon population densities in urban areas (e.g.11–15 raccoons per km^2 in Burlington; (Beasley et al., 2024; Prange et al., 2003; Rosatte et al., 2010; Slate et al., 2020). Furthermore, our choice of vaccination strategy may not be the most efficient for rabies prevention: we assigned an equal vaccination probability for all adult agents in the simulation, whereas previous work suggests that targeting preferred raccoon habitat is a more efficient vaccination strategy (McClure et al., 2022). Future work could investigate the efficacy of alternate vaccination strategies, such as spatially optimized baiting, on preventing recolonization. Regardless, vaccination is still an effective strategy for rabies elimination, and reducing the number of cases associated with recolonization events reduces the likelihood of dispersal of infected individuals to uninfected areas.

Our results suggest that immigration can sustain outbreaks in urban areas and influence rates of rabies recolonization. One of the limitations of our study is that the direction from which immigrants

arrive is stochastic: in reality, landscape characteristics such as connectivity likely result in directional differences in immigration rates (Algeo et al., 2017; Hopken, Mankowski, et al., 2025; Tardy et al., 2018), and the positioning of ORV zones relative to landscape features affects the direction from which infected immigrants could arrive (Rees et al., 2013; Russell et al., 2006). To use Burlington as an example, the city is bordered by Lake Champlain in the west and the Green Mountains in the east, therefore most raccoon movement likely occurs along a north-south axis. Furthermore, during the period when rabies was eliminated from greater Burlington and the surrounding area, rabies recolonization was only possible from south of the ORV zone. We chose not to account for geographic variation in immigration rates to make our results generalizable, but immigration rates and immigrant prevalence can be tailored to more accurately represent a city of interest. Future work for management applications could involve adjusting the landscape composition and immigration directions to generate more accurate assessments of rabies elimination and recolonization for specific cities in or near the ORV zone.

Due to longer enzootic periods due to low vaccination rates and susceptibility to rabies re-establishment, it is possible that urban areas located within ORV management zones may increase the risk of a barrier breach by acting as a “stepping stone” to regions in which raccoon rabies has been eliminated. The standard width of ORV zones in the United States is 40 km (McClure et al., 2020), which is larger than the majority of recorded raccoon dispersal distances (Rosatte et al., 2010). However, an ORV zone width of 40 km may be insufficient when infected individuals disperse from within the ORV zone due to a decrease in the distance an infected individual must travel to breach the barrier (McClure et al., 2020; Rees et al., 2013). The width of ORV zones intersecting an urban region may need to be increased to account for long-distance movements that originate within the zone, particularly when the urban region is located in a known risk corridor that facilitates long-distance raccoon movement (Algeo et al., 2017; Davis et al., 2019). Although adapting our model to a spatial extent to explore this ideas is computationally prohibitive, a potential next step is using a broader-scale

agent-based model such as the Ontario Rabies Model (Tinline et al., 2007) to test the stepping-stone hypothesis and evaluate the ability of increased ORV zone width to counteract potential stepping stone effects.

The dynamics of rabies re-emergence in regions where it has been eliminated depend on the timing and intensity of raccoon movement, as well as the origin of displaced raccoons. Immigrants from rural areas inside the ORV zone are more likely to be vaccinated than those from urban areas (Bigler et al., 2021; Gilbert et al., 2018; Johnson et al., 2021; Mainguy et al., 2012), and may represent a high enough proportion of immigrants to reduce recolonization risk. Furthermore, our results demonstrate that the intensity of immigration influences rabies dynamics. Given that raccoons are highly philopatric, with relatively short dispersal distances (Rees et al., 2008; Rosatte et al., 2010), immigration rates in this study may be artificially high. However, the paucity of movement data across the urban-rural interface make it difficult to accurately model immigration timing, intensity, and origin. Previous work using genetic methods successfully identified the origin of three raccoons which had undergone long-distance translocations (Hopken, Bjorklund, et al., 2025); but due the lack of clear population structure at finer geographic scales (Hopken et al., 2023; Root et al., 2009; but see Hopken, Mankowski, et al., 2025) it is unclear if these methods are useful for quantifying movement across localized urban-rural gradients. More data are needed to understand raccoon movements along urban-rural boundaries and the effects of these movements on rabies transmission.

Our results demonstrate that in urban-suburban landscapes with high raccoon population density, rabies elimination and subsequent recolonization is highly probable at small spatial extents. This work aligns with previous findings suggesting that rabies persistence is largely maintained on a regional scale (Biek et al., 2007; Fisher et al., 2018; Mancy et al., 2022; Smith et al., 2002). However, urban-suburban areas are still localized points of management concern, as low vaccination rates in these areas increase their potential as “stepping stones” that reduce the distance required to breach the

vaccination barrier. The potential for urban areas to amplify outbreak risk suggests the need for flexible, targeted management for both rabies elimination and prevention.

References

Acheson, E. S., Viard, F., Buchanan, T., Nituch, L., & Leighton, P. A. (2023). Comparing Control Intervention Scenarios for Raccoon Rabies in Southern Ontario between 2015 and 2025. *Viruses*, *15*(2), Article 2. https://doi.org/10.3390/v15020528

Algeo, T. P., Slate, D., Caron, R. M., Atwood, T., Recuenco, S., Ducey, M. J., Chipman, R. B., & Palace, M. (2017). Modeling Raccoon (Procyon lotor) Habitat Connectivity to Identify Potential Corridors for Rabies Spread. *Tropical Medicine and Infectious Disease*, *2*(3), 44. https://doi.org/10.3390/tropicalmed2030044

Bastille-Rousseau, G., Gorman, N. T., McClure, K. M., Nituch, L., Buchanan, T., Chipman, R. B., Gilbert, A. T., & Pepin, K. M. (2024). Assessing the Efficiency of Local Rabies Vaccination Strategies for Raccoons (Procyon lotor) in an Urban Setting. *Journal of Wildlife Diseases*, *60*(1). https://doi.org/10.7589/JWD-D-23-00059

Beasley, E. M., Nelson, K. M., Slate, D., Gilbert, A. T., Pogmore, F. E., Chipman, R. B., & Davis, A. J. (2024). Oral Rabies Vaccination of Raccoons (Procyon lotor) across a Development Intensity Gradient in Burlington, Vermont, USA, 2015–2017. *Journal of Wildlife Diseases*, *60*(1), 1–13. https://doi.org/10.7589/JWD-D-22-00117

Bettencourt, L. M. A., & Ribeiro, R. M. (2008). Real Time Bayesian Estimation of the Epidemic Potential of Emerging Infectious Diseases. *PLoS ONE*, *3*(5), e2185. https://doi.org/10.1371/journal.pone.0002185

Bezanson, J., Edelman, A., Karpinski, S., & Shah, V. B. (2017). Julia: A fresh approach to numerical computing. *SIAM Review*, *59*(1), 65–98.

Biek, R., Henderson, J. C., Waller, L. A., Rupprecht, C. E., & Real, L. A. (2007). A high-resolution genetic signature of demographic and spatial expansion in epizootic rabies virus. *Proceedings of the National Academy of Sciences*, *104*(19), 7993–7998. https://doi.org/10.1073/pnas.0700741104

Bigler, L. L., Ochwat, J. B., Scarpitta, S. C., Matthews, B. W., Rudd, R. J., & Lein, D. H. (2021). Virus neutralizing antibody following oral rabies vaccination of raccoons (Procyon lotor) on suburban Long Island, New York, USA. *The Journal of Wildlife Diseases*, *57*(1), 145–156.

Boelle, P.-Y., & Obadia, T. (2023). *R0: Estimation of R0 and Real-Time Reproduction Number from Epidemics* (Version 1.3-1) [R]. https://cran.r-project.org/web/packages/R0/index.html

Childs, J. E., Curns, A. T., Dey, M. E., Real, L. A., Feinstein, L., Bjørnstad, O. N., & Krebs, J. W. (2000). Predicting the local dynamics of epizootic rabies among raccoons in the United States. *Proceedings of the National Academy of Sciences*, *97*(25), 13666–13671. https://doi.org/10.1073/pnas.240326697

Cullingham, C. I., Pond, B. A., Kyle, C. J., Rees, E. E., Rosatte, R. C., & White, B. N. (2008). Combining direct and indirect genetic methods to estimate dispersal for informing wildlife disease management decisions. *Molecular Ecology*, *17*(22), 4874–4886. https://doi.org/10.1111/j.1365-294X.2008.03956.x

Davis, A. J., Kirby, J. D., Chipman, R. B., Nelson, K. M., & Gilbert, A. T. (2021). Data-Driven Management—A Dynamic Occupancy Approach to Enhanced Rabies Surveillance Prioritization. *Viruses*, *13*(9), Article 9. https://doi.org/10.3390/v13091795

Davis, A. J., Nelson, K. M., Kirby, J. D., Wallace, R., Ma, X., Pepin, K. M., Chipman, R. B., & Gilbert, A. T. (2019). Rabies Surveillance Identifies Potential Risk Corridors and Enables Management Evaluation. *Viruses*, *11*(11), Article 11. https://doi.org/10.3390/v11111006

Elmore, S. A., Chipman, R. B., Slate, D., Huyvaert, K. P., VerCauteren, K. C., & Gilbert, A. T. (2017). Management and modeling approaches for controlling raccoon rabies: The road to elimination.

PLOS Neglected Tropical Diseases, *11*(3), e0005249. https://doi.org/10.1371/journal.pntd.0005249

Etherington, T. R., Holland, E. P., & O'Sullivan, D. (2015). NLMpy: A python software package for the creation of neutral landscape models within a general numerical framework. *Methods in Ecology and Evolution*, *6*(2), 164–168. https://doi.org/10.1111/2041-210X.12308

Fehlner-Gardiner, C., Rudd, R., Donovan, D., Slate, D., Kempf, L., & Badcock, J. (2012). Comparing ONRAB And RABORAL V-RG oral rabies vaccine field performance in raccoons and striped skunks, New Brunswick, Canada, and Maine, USA. *Journal of Wildlife Diseases*, *48*(1), 157–167.

Fisher, C. R., Streicker, D. G., & Schnell, M. J. (2018). The spread and evolution of rabies virus: Conquering new frontiers. *Nature Reviews Microbiology*, *16*(4), 241–255. https://doi.org/10.1038/nrmicro.2018.11

Fournier, A., Fussell, D., & Carpenter, L. (1982). Computer rendering of stochastic models. *Communications of the ACM*, *25*(6), 371–384. https://doi.org/10.1145/358523.358553

Gilbert A, T. (2018). Rabies virus vectors and reservoir species. *Revue Scientifique et Technique (International Office of Epizootics)*, *37*(2), 371–384. https://doi.org/10.20506/rst.37.2.2808

Gilbert, A. T., Johnson, S. R., Nelson, K. M., Chipman, R. B., Algeo, T. P., Rupprecht, C. E., & Slate, D. (2018). Field trials of Ontario Rabies Vaccine bait in the northeastern USA, 2012–14. *Journal of Wildlife Diseases*, *54*(4), 790–801.

Grimm, V., Berger, U., Bastiansen, F., Eliassen, S., Ginot, V., Giske, J., Goss-Custard, J., Grand, T., Heinz, S. K., Huse, G., Huth, A., Jepsen, J. U., Jørgensen, C., Mooij, W. M., Müller, B., Pe'er, G., Piou, C., Railsback, S. F., Robbins, A. M., … DeAngelis, D. L. (2006). A standard protocol for describing individual-based and agent-based models. *Ecological Modelling*, *198*(1), 115–126. https://doi.org/10.1016/j.ecolmodel.2006.04.023

Grimm, V., Berger, U., DeAngelis, D. L., Polhill, J. G., Giske, J., & Railsback, S. F. (2010). The ODD protocol: A review and first update. *Ecological Modelling*, *221*(23), 2760–2768. https://doi.org/10.1016/j.ecolmodel.2010.08.019

Habib, T. J., Merrill, E. H., Pybus, M. J., & Coltman, D. W. (2011). Modelling landscape effects on density–contact rate relationships of deer in eastern Alberta: Implications for chronic wasting disease. *Ecological Modelling*, *222*(15), 2722–2732. https://doi.org/10.1016/j.ecolmodel.2011.05.007

Haley, B. S., Berentsen, A. R., & Engeman, R. M. (2019). Taking the bait: Species taking oral rabies vaccine baits intended for raccoons. *Environmental Science and Pollution Research*, *26*(10), 9816–9822. https://doi.org/10.1007/s11356-019-04200-7

Hampson, K., Dushoff, J., Cleaveland, S., Haydon, D. T., Kaare, M., Packer, C., & Dobson, A. (2009). Transmission Dynamics and Prospects for the Elimination of Canine Rabies. *PLoS Biology*, *7*(3), e1000053. https://doi.org/10.1371/journal.pbio.1000053

Hanlon, C. A., Niezgoda, M., & Rupprecht, C. E. (2007). 5—Rabies in Terrestrial Animals. In A. C. Jackson & W. H. Wunner (Eds.), *Rabies (Second Edition)* (pp. 201–258). Academic Press. https://doi.org/10.1016/B978-012369366-2/50007-5

Hesselbarth, M. H. K., Sciaini, M., With, K. A., Wiegand, K., & Nowosad, J. (2019). landscapemetrics: An open-source R tool to calculate landscape metrics. *Ecography*, *42*(10), 1648–1657. https://doi.org/10.1111/ecog.04617

Homer, C., Dewitz, J., Yang, L., Jin, S., Danielson, P., Xian, G., Coulston, J., Herold, N., Wickham, J., & Megown, K. (2015). Completion of the 2011 National Land Cover Database for the Conterminous United States – Representing a Decade of Land Cover Change Information. *Photogrammetric Engineering & Remote Sensing*, *81*(5), 345–354. https://doi.org/10.1016/S0099-1112(15)30100-2

Hopken, M. W., Bjorklund, B., Mankowski, C. C. P., Kirby, J., Chipman, R. B., Buchanan, T., Nituch, L., Gagnier, M., Massé, A., & Gilbert, A. T. (2025). Tracking the Origin of Raccoon (Procyon

lotor) Translocations in Northeastern North America Using Population Genetics. *Northeastern Naturalist*, *31*(4), 539–554. https://doi.org/10.1656/045.031.0412

Hopken, M. W., Mankowski, C. P., Thurber, C., Piaggio, A. J., Nelson, K. M., Chipman, R. B., Abdo, Z., Buchanan, T., Massé, A., & Gilbert, A. T. (2025). Contrasting Patterns of Raccoon (Procyon lotor) Spatial Population Genomics Throughout a Rabies Management Area in Eastern North America. *Evolutionary Applications*, *18*(5), e70105. https://doi.org/10.1111/eva.70105

Hopken, M. W., Piaggio, A. J., Abdo, Z., Chipman, R. B., Mankowski, C. P., Nelson, K. M., Hilton, M. S., Thurber, C., Tsuchiya, M. T. N., Maldonado, J. E., & Gilbert, A. T. (2023). Are rabid raccoons (Procyon lotor) ready for the rapture? Determining the geographic origin of rabies virus-infected raccoons using RADcapture and microhaplotypes. *Evolutionary Applications*, *16*(12), 1937–1955. https://doi.org/10.1111/eva.13613

Jenkins, S. R., Perry, B. D., & Winkler, W. G. (1988). Ecology and Epidemiology of Raccoon Rabies. *Reviews of Infectious Diseases*, *10*(Supplement_4), S620–S625. https://doi.org/10.1093/clinids/10.Supplement_4.S620

Johnson, S. R., Slate, D., Nelson, K. M., Davis, A. J., Mills, S. A., Forbes, J. T., VerCauteren, K. C., Gilbert, A. T., & Chipman, R. B. (2021). Serological responses of raccoons and striped skunks to Ontario rabies vaccine bait in West Virginia during 2012–2016. *Viruses*, *13*(2), 157.

Kirby, J. D., Chipman, R. B., Nelson, K. M., Rupprecht, C. E., Blanton, J. D., Algeo, T. P., & Slate, D. (2017). Enhanced rabies surveillance to support effective oral rabies vaccination of raccoons in the eastern United States. *Tropical Medicine and Infectious Disease*, *2*(3), 34.

Li, M., Roswell, M., Hampson, K., Bolker, B. M., & Dushoff, J. (2024). *Reassessing global historical $\mathscr{R}_0$ estimates of canine rabies*. https://doi.org/10.1101/2024.04.11.589097

Lotze, J.-H., & Anderson, S. (1979). Procyon lotor. *Mammalian Species*, (119), 1–8.

Ma, X., Monroe, B. P., Wallace, R. M., Orciari, L. A., Gigante, C. M., Kirby, J. D., Chipman, R. B., Fehlner-Gardiner, C., Cedillo, V. G., Petersen, B. W., Olson, V., & Bonwitt, J. (2021). Rabies surveillance in the United States during 2019. *Journal of the American Veterinary Medical Association*, *258*(11), 1205–1220. https://doi.org/10.2460/javma.258.11.1205

Mainguy, J., Rees, E. E., Canac-Marquis, P., Bélanger, D., Fehlner-Gardiner, C., Séguin, G., Larrat, S., Lair, S., Landry, F., & Côté, N. (2012). Oral rabies vaccination of raccoons and striped skunks with ONRAB® baits: Multiple factors influence field immunogenicity. *Journal of Wildlife Diseases*, *48*(4), 979–990.

Mancy, R., Rajeev, M., Lugelo, A., Brunker, K., Cleaveland, S., Ferguson, E. A., Hotopp, K., Kazwala, R., Magoto, M., Rysava, K., Haydon, D. T., & Hampson, K. (2022). Rabies shows how scale of transmission can enable acute infections to persist at low prevalence. *Science*, *376*(6592), 512–516. https://doi.org/10.1126/science.abn0713

McClure, K. M., Bastille-Rousseau, G., Davis, A. J., Stengel, C. A., Nelson, K. M., Chipman, R. B., Wittemyer, G., Abdo, Z., Gilbert, A. T., & Pepin, K. M. (2022). Accounting for animal movement improves vaccination strategies against wildlife disease in heterogeneous landscapes. *Ecological Applications*, *32*(4), e2568.

McClure, K. M., Gilbert, A. T., Chipman, R. B., Rees, E. E., & Pepin, K. M. (2020). Variation in host home range size decreases rabies vaccination effectiveness by increasing the spatial spread of rabies virus. *Journal of Animal Ecology*, *89*(6), 1375–1386. https://doi.org/10.1111/1365-2656.13176

Ontario Ministry of Natural Resources and Forestry. (2025, April 14). *Wildlife rabies outbreaks and control operations*. http://www.ontario.ca/page/wildlife-rabies-outbreaks-and-control-operations

Poisot, T., Borregaard, M. K., Catchen, M. D., Schouten, R., & Baudrot, V. (2023). *NeutralLandscapes* (Version 0.1.3) [Julia]. https://docs.ecojulia.org/NeutralLandscapes.jl/dev/

Prange, S., & Gehrt, S. D. (2004). Changes in mesopredator-community structure in response to urbanization. *Canadian Journal of Zoology*, *82*(11), 1804–1817. https://doi.org/10.1139/z04-179

Prange, S., Gehrt, S. D., & Wiggers, E. P. (2003). Demographic factors contributing to high raccoon densities in urban landscapes. *The Journal of Wildlife Management*, 324–333.

Prange, S., Gehrt, S. D., & Wiggers, E. P. (2004). Influences of anthropogenic resources on raccoon (Procyon lotor) movements and spatial distribution. *Journal of Mammalogy*, *85*(3), 483–490.

Randa, L. A., & Yunger, J. A. (2006). Carnivore occurrence along an urban-rural gradient: A landscape-level analysis. *Journal of Mammalogy*, *87*(6).

Recuenco, S., Eidson, M., Kulldorff, M., Johnson, G., & Cherry, B. (2007). Spatial and temporal patterns of enzootic raccoon rabies adjusted for multiple covariates. *International Journal of Health Geographics*, *6*(1), 14. https://doi.org/10.1186/1476-072X-6-14

Rees, E. E., Pond, B. A., Phillips, J. R., & Murray, D. (2008). Raccoon ecology database: A resource for population dynamics modelling and meta-analysis. *Ecological Informatics*, *3*(1), 87–96. https://doi.org/10.1016/j.ecoinf.2008.01.002

Rees, E. E., Pond, B. A., Tinline, R. R., & Bélanger, D. (2013). Modelling the effect of landscape heterogeneity on the efficacy of vaccination for wildlife infectious disease control. *Journal of Applied Ecology*, *50*(4), 881–891. https://doi.org/10.1111/1365-2664.12101

Reynolds, J. J. H., Hirsch, B. T., Gehrt, S. D., & Craft, M. E. (2015). Raccoon contact networks predict seasonal susceptibility to rabies outbreaks and limitations of vaccination. *Journal of Animal Ecology*, *84*(6), 1720–1731. https://doi.org/10.1111/1365-2656.12422

Root, J. J., Puskas, R. B., Fischer, J. W., Swope, C. B., Neubaum, M. A., Reeder, S. A., & Piaggio, A. J. (2009). Landscape Genetics of Raccoons (Procyon lotor) Associated with Ridges and Valleys of Pennsylvania: Implications for Oral Rabies Vaccination Programs. *Vector-Borne and Zoonotic Diseases*, *9*(6), 583–588. https://doi.org/10.1089/vbz.2008.0110

Rosatte, R., Donovan, D., Allan, M., Bruce, L., Buchanan, T., Sobey, K., Stevenson, B., Gibson, M., MacDonald, T., Whalen, M., Davies, J. C., Muldoon, F., & Wandeler, A. (2009). The control of raccoon rabies in Ontario, Canada: Proactive and reactive tactics, 1994–2007. *Journal of Wildlife Diseases*, *45*, 772–784.

Rosatte, R., Ryckman, M., Ing, K., Proceviat, S., Allan, M., Bruce, L., Donovan, D., & Davies, J. C. (2010). Density, movements, and survival of raccoons in Ontario, Canada: Implications for disease spread and management. *Journal of Mammalogy*, *91*(1), 122–135. https://doi.org/10.1644/08-MAMM-A-201R2.1

Rosatte, R., Sobey, K., Donovan, D., Bruce, L., Allan, M., Silver, A., Bennett, K., Gibson, M., Simpson, H., & Davies, C. (2006). Behavior, movements, and demographics of rabid raccoons

in Ontario, Canada: Management implications. *Journal of Wildlife Diseases*, *42*(3), 589–605.

Roscoe, D. E., Holste, W. C., Sorhage, F. E., Campbell, C., Niezgoda, M., Buchannan, R., Diehl, D., Niu, H. S., & Rupprecht, C. E. (1998). EFFICACY OF AN ORAL VACCINIA-RABIES GLYCOPROTEIN RECOMBINANT VACCINE IN CONTROLLING EPIDEMIC RACCOON RABIES IN NEW JERSEY. *Journal of Wildlife Diseases*, *34*(4), 752–763. https://doi.org/10.7589/0090-3558-34.4.752

Rupprecht, C. E., Hanlon, C. A., & Hemachudha, T. (2002). Rabies re-examined. *The Lancet Infectious Diseases*, *2*(6), 327–343. https://doi.org/10.1016/S1473-3099(02)00287-6

Russell, C. A., Real, L. A., & Smith, D. L. (2006). Spatial Control of Rabies on Heterogeneous Landscapes. *PLoS ONE*, *1*(1), e27. https://doi.org/10.1371/journal.pone.0000027

Signer, J., Fieberg, J., & Avgar, T. (2017). Estimating utilization distributions from fitted step-selection functions. *Ecosphere*, *8*(4), e01771. https://doi.org/10.1002/ecs2.1771

Slate, D., Chipman, R. B., Algeo, T. P., Mills, S. A., Nelson, K. M., Croson, C. K., Dubovi, E. J., Vercauteren, K., Renshaw, R. W., Atwood, T., Johnson, S., & Rupprecht, C. E. (2014). Safety and immunogenicity of Ontario Rabies Vaccine Bait (ONRAB) in the first US field trial in raccoons (Procyon lotor). *Journal of Wildlife Diseases*, *50*(3), 582–595. https://doi.org/10.7589/2013-08-207

Slate, D., Saidy, B. D., Simmons, A., Nelson, K. M., Davis, A., Algeo, T. P., Elmore, S. A., & Chipman, R. B. (2020). Rabies Management Implications Based on Raccoon Population Density Indexes. *The Journal of Wildlife Management*, *84*(5), 877–890. https://doi.org/10.1002/jwmg.21869

Smith, D. L., Lucey, B., Waller, L. A., Childs, J. E., & Real, L. A. (2002). Predicting the spatial dynamics of rabies epidemics on heterogeneous landscapes. *Proceedings of the National Academy of Sciences*, *99*(6), 3668–3672. https://doi.org/10.1073/pnas.042400799

Tardy, O., Massé, A., Pelletier, F., & Fortin, D. (2018). Interplay between contact risk, conspecific density, and landscape connectivity: An individual-based modeling framework. *Ecological Modelling*, *373*, 25–38. https://doi.org/10.1016/j.ecolmodel.2018.02.003

Tinline, R., Ball, D., Broadfoot, J., & Pond, B. (2007). The Ontario rabies model. *Queens University, Kingston, Ontario, Canada*.

Tinline, R., Rosatte, R., & MacInnes, C. (2002). Estimating the incubation period of raccoon rabies: A time–space clustering approach. *Preventive Veterinary Medicine, Spatial Epidemiology*, *56*(1), 89–103. https://doi.org/10.1016/S0167-5877(02)00126-5

Townsend, S. E., Sumantra, I. P., Pudjiatmoko, Bagus, G. N., Brum, E., Cleaveland, S., Crafter, S., Dewi, A. P. M., Dharma, D. M. N., Dushoff, J., Girardi, J., Gunata, I. K., Hiby, E. F., Kalalo, C., Knobel, D. L., Mardiana, I. W., Putra, A. A. G., Schoonman, L., Scott–Orr, H., … Hampson, K. (2013). Designing Programs for Eliminating Canine Rabies from Islands: Bali, Indonesia as a Case Study. *PLOS Neglected Tropical Diseases*, *7*(8), e2372. https://doi.org/10.1371/journal.pntd.0002372

Vander Wal, E., Laforge, M. P., & McLoughlin, P. D. (2014). Density dependence in social behaviour: Home range overlap and density interacts to affect conspecific encounter rates in a gregarious ungulate. *Behavioral Ecology and Sociobiology*, *68*(3), 383–390. https://doi.org/10.1007/s00265-013-1652-0

Vercauteren, K. C., Ellis, C., Chipman, R., DeLiberto, T. J., Shwiff, S. A., & Slate, D. (2012). Rabies in North America: A Model of the One Health Approach. *Wildlife Diseases*.

Vermont Department of Health. (2025, March). *2024 Rabies Surveillance Report*. https://www.healthvermont.gov/sites/default/files/document/lsid-2024-rabies-surveillance-report.pdf

Viard, F., Acheson, E., Allibert, A., Sauve, C., & Leighton, P. (2022). *SamPy: A New Python Library for Stochastic Spatial Agent-Based Modeling in Epidemiology of Infectious Diseases* (No. 2022110556). Preprints. https://doi.org/10.20944/preprints202211.0556.v2

White, L. F., Wallinga, J., Finelli, L., Reed, C., Riley, S., Lipsitch, M., & Pagano, M. (2009). Estimation of the reproductive number and the serial interval in early phase of the 2009 influenza A/H1N1 pandemic in the USA. *Influenza and Other Respiratory Viruses*, *3*(6), 267–276. https://doi.org/10.1111/j.1750-2659.2009.00106.x

Yang, A., Boughton, R., Miller, R. S., Snow, N. P., Vercauteren, K. C., Pepin, K. M., & Wittemyer, G. (2023). Individual-level patterns of resource selection do not predict hotspots of contact. *Movement Ecology*, *11*(1), 74. https://doi.org/10.1186/s40462-023-00435-9

Figures and Tables

Figure 1. Transitions between susceptible (S), exposed (E), infected (I), and recovered (R) disease states of the model. Transitions between states are governed by probability of vaccination (v, 0–80% annually), force of infection (λ, which varies spatially), and weekly infectious probability (δ, which varies with time spent in the exposed state). Agents in the exposed state have an 8–12% probability of transitioning to the recovered rather than the infectious state. Demographic processes include birth (b), immigration (i), emigration (e), and death (d; all infectious agents die after 1 week).

Figure 2. Proportion of simulations in which the initial rabies outbreak was eliminated. Rabies was more likely to be eliminated in simulations where adult vaccination rates were high, immigration rates (measured in terms of the expected number of weekly immigrants) were low (a), and disease rates within immigrants were low (b). Simulations with vaccination rates were also more resistant to increases in immigration variables, as shown by the smaller decrease in elimination probability with higher immigration rates.

Figure 3. Time until rabies elimination (in years) in simulations where rabies was eliminated at least once. Numbers represent elimination probability at a given vaccination rate. Simulations with higher adult vaccination rates reached elimination more quickly: simulations with adult vaccination rates of 50% or higher had a median elimination time of less than 1.5 years; whereas simulations with vaccination rates of 0–10% had a median elimination time of greater than 3 years.

Figure 4. Expected weekly immigrants, immigrant disease rate (i.e. the probability an immigrant was infected with rabies), and adult vaccination rate influenced the weekly probability of rabies

recolonization. Recolonization probability increased by 0.6% with each additional weekly immigrant (a,b), and by 0.16% with each 1% increase in immigrant disease rate (a). Each 10% increase in adult vaccination rate decreased weekly recolonization probability by 0.16%, predominantly by reducing the likelihood of unusually high weekly recolonization probabilities above the interquartile range (c). There was no clear effect of immigration type on weekly recolonization probability (b). Outliers removed for clarity.

Acknowledgments. We thank Amy Davis and Kim Pepin for their helpful advice on our methodology; and two anonymous reviewers for their feedback on the manuscript. This research was funded by award 223764/Z/21/Z from the Wellcome Trust and a National Science Foundation (NSF) Biology Integration Institute grant (DBI 2213854) to the Verena program (viralemergence.org).

Conflict of Interest. The authors have no conflicts of interest to declare.

Author Contributions. E.M. Beasley analyzed and interpreted the analysis and results and drafted the manuscript. Both authors contributed to the conception and design of the project, contributed critically to the manuscript drafts, revised the manuscript and gave approval for publication.

Statement of Inclusion. The authors received and implemented feedback from colleagues at rabies-managing governmental agencies throughout the design and analysis portions of this research. We have communicated our results to rabies managers at professional conferences and will continue to disseminate the results to relevant rabies-managing agencies in our region.

Data Availability Statement. The associated repository will be archived and made publicly available on Zenodo upon acceptance of the manuscript.

Appendix 1: Expanded Methodology and Model Specifications

The model description herein follows the ODD (Overview, Design concepts, Details) protocol for describing individual-based models, including agent-based models (Grimm et al., 2006, 2010).

Overview

I. *Purpose.*

We used this agent-based model to describe the effects of vaccine-induced immunity and immigration on rabies dynamics in a simulated urban-suburban landscape. Although immigration is likely responsible for the recent re-emergence of rabies cases in Chittenden County, Vermont, data on immigration and emigration in urban areas is sparse and the effects of these processes on rabies dynamics is poorly understood. Because of the relative scarcity of work investigating the role of immigration in sustaining and re-establishing rabies in urban areas, we used this model to provide a baseline understanding of these processes. We designed the model to be flexible enough to incorporate more complex scenarios, such as variability in individual habitat selection behavior or more realistic vaccination scenarios.

II. *Entities, state variables, and scales*

The model consisted of two entities: agents and grid cells. Each grid cell represented a 0.5 x 0.5 km^2 section of the landscape and contained the attributes habitat type (e.g. forest, low urban development, pasture, etc.) and a vaccination probability for agents over 52 weeks of age. Each agent represented a raccoon and has a variety of attributes (Table 1-1).

Table 1-1. Attributes of simulated agents.

Attribute	Description
ID	Unique identifier for each agent
Position	Coordinates of agent at time step *t*
Home Range Attractor	Coordinates of the agent's home range attractor
Incubation	Binary indicator of the agent's disease state. 0 = uninfected, 1 = infected with rabies
Time since infection	If incubation = 1, the number of weeks since the agent entered the incubation state
Contagious	If incubation = 1, binary indicator of the agent's contagious state. 0 = not contagious (i.e. cannot spread disease), 1 = contagious
Time since contagious	If contagious = 1, the number of weeks since the agent entered the contagious state
Sex	Sex of each agent; 0 = male, 1 = female
Mother	ID of the agent's mother
Immunity	Binary indicator of an agent's immunity status, 0 = not immune to disease, 1 = immune to disease
Age	Age of the agent in weeks

The model landscape consisted of a 60 x 60 square grid, for a total simulation area of approximately 30 km x 30 km. The boundaries of the landscape were reflective, i.e. agents generally could not leave the landscape (see the dispersal submodel in section VII: Submodels for exceptions). Each time step represented 1 week and simulations were run for 11 years, with 52 time steps per year.

III. *Process overview and scheduling*

Time in the simulations was modeled as discrete 1-week steps. Grid cell attributes were fixed for the duration of each simulation, but agent attributes could be changed weekly, or during particular time steps within each year (i.e. seasonally). The first year of the 11-year simulation was treated as a burn-in period to allow the agent population to stabilize before the disease was introduced (i.e. a unique event). The full model schedule can be found in Table 1-2.

Table 1-2. Scheduling of model processes. Within frequency categories, processes are presented in the order in which they occur. Immigration timing varied depending on the simulated scenario and either occurred weekly (consistent immigration) or seasonally.

Frequency	Time step	Event	Description
Weekly		Mortality	Agents are removed from the simulation due to stochastic, old age, disease-induced, and carrying capacity-induced mortality
		Movement	Agents' weekly positions are updated
		Disease transmission	Contagious agents can infect new agents
		Immigration (consistent)	New agents over 52 weeks of age which are not associated with any existing agents are added to the simulation
		Disease state change	Agents which are infected can become contagious or can shed the infection and immune. Time since infection and time since contagious attributes increase by 1
Seasonally	Week 18	Reproduction	New agents with age 0 that are associated with existing female agents are added to the simulation
	Week 35	Vaccination	Agents which are not immune can become immune
	Weeks 41–45	Dispersal	Agents' home range attractor can be updated; if the new home range attractor is outside of the landscape boundary, the agent is removed from the simulation
	Week 40-50	Immigration (seasonal)	New agents over 52 weeks of age which are not associated with any existing agents are added to the simulation
Unique	Year 2, Week 1	Disease initialized	10 agents are randomly selected from non-immune agents and become infected

Design Concepts

IV. *Design Concepts*

Basic Principles. We designed our agent-based model as a spatially explicit SEIR model, with additional demographic processes such as births, deaths, immigration, and emigration (Figure 1-1). The spatially explicit component of the model primarily affects the force of infection parameter λ, which varies based on the proximity of an agent to a contagious agent (Figure 1-2). The spatially explicit component of the model also influences the demographic parameters *e* (emigration) and *d* (death) due to increased mortality rates and increased probability of dispersal (therefore increasing the likelihood of an agent leaving the landscape) in grid cells in which the number of agents exceeds the carrying capacity.

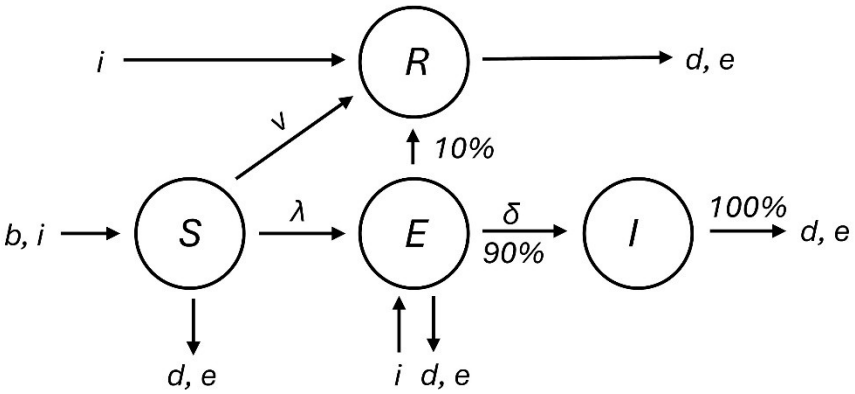

Figure 1-1. Transitions between susceptible (S), exposed (E), infected (I), and recovered (R) disease states of the model. Transitions between disease states are governed by probability of vaccination (*v*, 0–80% annually), force of infection (λ, which varies spatially), and weekly infectious probability (δ, which varies with time spent in the exposed state). Approximately 90% of exposed individuals eventually transition to the infectious state; approximately 10% instead transition to the recovered state. Demographic processes include birth (*b*), immigration (*i*), emigration (e), and death (*d*; all agents in the infectious state die after 1 week).

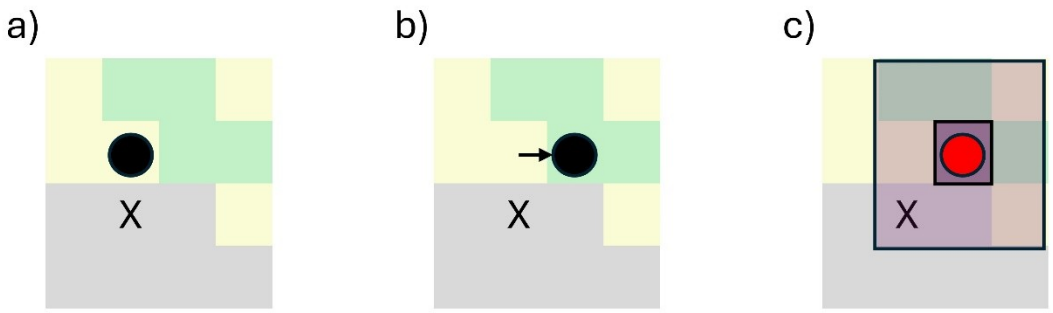

Figure 1-2. a) Each agent in the model is assigned a home range attractor (black X), which can change during the annual dispersal period, and a position (black circle), which can change each week. The agent's weekly position (b) is selected from the previous position's Moore (9-cell) neighborhood, with the probability of selection weighted based on the habitat type, distance from the home range attractor, and the number of agents in each of the possible target cells. If the agent is in the infectious period of the disease (c, red circle), it can infect agents within 500 m of its current position with a probability λ_1. Agents within 1 km of the infected agent's position are infected with a lower probability λ_2.

The disease and demographic processes are heavily influenced by the movement of individual agents in the simulation landscape. Movements can be categorized into two types: weekly and seasonal movements. Weekly movements result in changes in an agent's weekly position in the landscape and are influenced by the habitat type, number of agents, and distance from the agent's home range attractor of each grid cell in the agent's Moore (9-cell) neighborhood. Agents can also disperse seasonally (i.e. update the location of their home range attractor). Agents less than 52 weeks of age always undergo the dispersal process; however, their dispersal distance can be 0, effectively representing an agent that does not disperse from its natal home range. Agents over 52 weeks of age can disperse if the number of agents in the agent's current cell exceeds the cell's carrying capacity. Similarly to agents less than 52 weeks of age, the dispersal distance can be 0. For more details, see the movement submodel in Section VII: Submodels.

Interactions. Direct interactions between agents influence disease transmission and agent movement. For weekly agent movement, an agent's weekly position is influenced by the number of agents in a given cell within movement range, among other factors. Agents less than 20 weeks of age always inhabit the same cell as their mother. On a seasonal basis, agents over 52 weeks of age can disperse if the number of agents in their current position exceeds the carrying capacity of that cell. Interactions between agents are also assumed, but not explicitly defined, in the disease transmission submodel. A contagious agent can transmit the disease to agents within 500 m of the infectious agent's position with a given probability λ_1, and can transmit the disease to agents within 1 km of the agent's current position with a probability λ_2 (Figure 1-2). These values were chosen based on the results of a parameter sensitivity analysis (Appendix 2). In both cases, it assumed that the contagious agent must have contact with another agent in order to spread the disease, given that rabies is transmitted via direct contact. See the disease transmission submodel in Section VII: Submodels for more details.

Stochasticity. Most processes in the model are at least partially stochastic. The biological realities these processes represent are often highly variable, and the causes of this variability are not always understood. We are more interested in exploring the consequences of this variability rather than its causes: e.g., we are interested in how varying immigration rates influence rabies persistence, but not necessarily in the biological mechanisms leading to changes in immigration rates. Therefore, we have used stochasticity to generate variability in parameter values and processes that roughly matches the variability observed in real systems. For specific information on how stochasticity is implemented in specific processes, see Section VII: Submodels.

Details

V. *Initialization*

Landscape initialization. We initialized the 60 x 60 landscape using the midpoint displacement algorithm in the Neutral Landscapes package in Julia (Etherington et al., 2015; Fournier et al., 1982).

We supplied an autocorrelation parameter that matches the landscape autocorrelation of the greater Burlington, Vermont, area; upon which our simulations are loosely based (see Section VI: Inputs for details). We then reclassified the landscape into discrete habitat categories, the relative proportions of which matched the land cover composition of Burlington. We then created a 5-cell zone of a unique "buffer" habitat on the outer sides of the simulated landscape. The purpose of the buffer is twofold: 1) to reduce the effects of artificial boundaries in the simulated landscape (see the movement submodel in Section VII: Submodels) and 2) to represent the rural landscape surrounding the greater Burlington area, which differs in raccoon density, movement patterns, and vaccine-induced immunity rates (Bastille-Rousseau et al., 2024; Fehlner-Gardiner et al., 2012; Prange et al., 2004).

Initializing agents. We populated non-buffer cells of the simulated landscape using a Poisson point process in which the expected number of agents per cell (λ) was 1.5. All disease-related attributes were set to 0 (i.e. no agent had contracted the disease). Agent sex and age were stochastically assigned: each agent had a 50% probability of being male or female, whereas each agent's age in weeks was randomly selected from a range of 52–416 weeks (the maximum age in the simulation). Immunity status was assigned as the outcome of a Bernoulli trial, in which the probability of an agent being immunized varied based on the user-defined vaccination probability. Buffer cells were populated using the same procedure, but with a lower expected number of agents per cell ($\lambda = 1$) and a fixed probability of disease immunity (0.6). The initial vaccination probability in the buffer zone is based on the USDA's target vaccine-induced immunity rates, which is frequently achieved in rural areas (Fehlner-Gardiner et al., 2012; Johnson et al., 2021).

VI. *Inputs*

We simulated landscapes based on NLCD land cover data from the greater Burlington, Vermont area (Homer et al., 2015). We obtained land cover at a 30m x 30m resolution from the NLCD website and trimmed the raster to an extent of -73.347 – -73.0.17 degrees longitude and 44.374 – 44.587

degrees latitude. We reclassified the land cover data based on land cover categories used in the National Rabies Management Program Oral Rabies Vaccine baiting algorithm (McClure et al., 2022). After land cover reclassification, we calculated 1) the proportion of each land cover type in the landscape and 2) a spatial autocorrelation index using the function `lsm_l_ai` in the R package `landscapemetrics` (Hesselbarth et al., 2019). The land cover proportions and autocorrelation index were used to generate simulated landscapes.

VII. *Submodels*

The following submodels are presented in the order in which they occur in the simulation.

Mortality. There were several sources of mortality, in which agents were removed from the landscape. Each week, agents could be stochastically removed from the landscape with a probability of 0.001, which represented all potential sources of mortality that were not explicitly defined here (e.g., vehicle collisions). All agents in the contagious state of the disease died after having been in the contagious state for 2 weeks. Because disease mortality occurs before disease transmission in each time step, this corresponds to 1 week in which the agent can potentially spread the disease to other agents. Agents were removed from the simulation upon reaching 416 weeks (8 years) of age. Finally, agents with a weekly position in a cell that exceeded carrying capacity were subjected to higher weekly mortality rates: agents at least 52 weeks of age had a carrying capacity mortality rate of 0.005, whereas agents younger than 52 weeks of age had a carrying capacity mortality rate of 0.02. These differential mortality rates lead to increased mortality among younger agents, which is observed in real populations (Pitt et al., 2008).

Movement. Each agent in the simulation can potentially update their weekly position. For agents at least 20 weeks of age (i.e. agents old enough to move independently of their mother), each agent selected a position from within the current cell's 9-cell (Moore) neighborhood, which includes the agent's current position and the eight adjacent landscape cells. These cells were selected using a

weighted probability that accounted for 1) the habitat type in each cell, 2) the distance from the agent's home range attractor, and 3) the number of agents occupying each cell in the previous time step. We weighted each component process independently, then calculated the final weight as a product of the three processes. Weighted probabilities were calculated using the `Weights` function in the StatsBase package in Julia v. 1.9.2 (Bezanson et al., 2017).

To account for habitat type in each agent's weekly movement, we used resource selection function (RSF) coefficients calculated by McClure et al. (2022) as the values for each weighted probability calculation. We used population-level coefficients rather than individual-level coefficients to calculate movement probabilities: a decision which omits the individual variability found in real populations, which may in turn influence disease dynamics. However, reducing individual variability in movement reduces some of the "noise" from this variability, allowing us to focus on the effects of immigration and population-level immunity. We accounted for distance from an agent's home range attractor using methods derived from Signer et al. (2017) (Eq. 1-1):

$$p(c_{t+1}) \propto \exp(-\omega d(c_{t+1})) \quad \text{(Eq. 1-1)}$$

In which $p(c_t)$ the probability of a raccoon occupying cell c within the raccoon's current Moore neighborhood at time $t+1$, ω the strength of attraction towards the location of the home range attractor, and $d(c_t)$ the squared distance between potential target cells and the home cell. The squared distance between cells was calculated by (Eq. 1-2):

$$d(c_t) = \frac{r((x_t - x_h)^2 + (y_t - y_h)^2)}{100} \quad \text{(Eq. 1-2)}$$

After agents at least 20 weeks old selected their weekly position, the position of any agents less than 20 weeks old was updated to match their mother's.

Disease transmission. Only agents in the infectious state of the disease could transmit the disease (Figure 1-1). Furthermore, these agents could only transmit the disease to agents within 1 km of their current weekly position which had not acquired immunity through vaccination or recovery from

the exposed state. Disease transmission had a spatial component (Figure 1-2) in which agents had a higher probability of transmitting the disease to agents within 500 m of their current position (λ_1) than to agents within 1 km of their current position (λ_2). These probabilities were selected using a parameter sensitivity analysis (Appendix 2). Although it is more common to use a continuous distance-decay function to account for spatial effects on disease transmission, the grain size of the simulation (0.5 x 0.5 km) compared to the typical weekly home range size of raccoons in urban-suburban landscapes such as Burlington (mean radius 600m, McClure et al., 2022) would essentially result in discrete transmission probabilities. We supplied these probabilities based on the results of a parameter sensitivity analysis rather than calculating them each time step to reduce computation time.

Change disease state. Each week, an agent in the exposed state of the disease could recover from the disease with a probability of 0.002. Recovered agents obtained lifelong immunity to the disease. Agents which did not recover transitioned to the infectious state with a probability drawn from a beta distribution $P \sim Beta(t, 5)$, in which t is the number of weeks since the agent was exposed to the disease. These weekly probabilities resulted in a total probability of recovery of 8–12% and a typical disease incubation period of 4–6 weeks, which is consistent with observed values (see Appendix 2 for details).

Update temporal attributes. Each agent's age, time since infection (if in the exposed state), and time since entering the infectious state (if in the infectious state) was increased by 1 each week.

Immigration. Immigration could occur either weekly (consistent immigration) or seasonally. When immigration was set to be consistent, the number of immigrants per week was drawn from a Poisson distribution $N \sim Pois(n)$, in which n took values of 1–5 expected immigrants per week. Most immigrant attributes were assigned the same way as the initial population (see Section V: Initialization); with the exception of the agents' position, immunity status, and incubation status. Each agent immigrating into the landscape was assigned an initial position along one of the edges of the simulated landscape. Each immigrating agent could be incubating the disease with a user-defined

probability which could take values of 0, 0.015, 0.03, 0.045, and 0.06. All immigrants were assumed to have an immunity status of 0. After attributes were assigned, immigrants were randomly assigned a movement direction that would not immediately take them out of the simulated landscape, and a movement distance. Agents then moved to a new position based on these parameters.

Seasonal immigration took place between weeks 40 and 50 of the simulation. The procedure is the same as consistent immigration, with the exception that the number of weekly immigrants was determined by $N \sim Pois(n*5)$, which resulted in approximately the same total number of immigrants for the duration of each simulation (Appendix 2).

Reproduction. Reproduction occurred at week 18 of each year in the simulation. Female agents were randomly selected to reproduce with a probability of 95% (Rees et al., 2013; Tinline et al., 2007). We then assigned the number of offspring for each reproducing female by drawing from a Poisson distribution $N_i \sim Pois(4)$, in which N_i was the number of offspring produced by agent i. With this distribution a litter size of 0 was possible, but rare. Each offspring was assigned a value of male or female with a 50% probability and its initial position was the same as the mother's. Offspring were also assigned a unique identifier and all disease and vaccination states were set at 0. Although it is likely that immune female raccoons confer some rabies immunity to their offspring, we did not incorporate this into the model because the duration and strength of rabies resistance conferred this way is currently unknown (Fry et al., 2013).

Vaccination. Vaccination success of a given agent during the annual vaccination period (week 35) was based on the agent's age and position. Agents in the buffer zone which were at least 1 year old had a vaccination probability of 60%, consistent with empirical vaccination rates in rural areas (Fehlner-Gardiner et al., 2012). Agents elsewhere in the landscape that were at least 1 year old were vaccinated with a user-defined probability that ranged from 0–80% at 10% intervals. Agents less than 1 year old had a vaccination probability that was half of the probability for agents older than 1 year (Beasley et al., 2024).

Dispersal. Seasonal dispersal as defined here includes a potential change in 1) the agent's current position and 2) the location of an agent's home range attractor. The dispersal function was activated from weeks 41–45 of each year of the simulation and was largely the same for raccoons of all ages. Starting from the agent's current position, each agent undergoing dispersal was assigned a movement direction and distance. Movement direction was defined by randomly selecting one of the eight cells in the agent's Moore neighborhood (Cullingham et al., 2008). Movement distance was defined as the number of landscape cells traveled and was drawn from a Poisson distribution with an expected movement distance λ that varied based on the agent's age (it was possible for any agent to have a movement distance of 0). The agents then moved to a new position according to their assigned movement distance and direction. Agents whose updated position fell outside of the landscape boundary were permanently deleted from the simulation. All other agents' home range attractor was updated to the agents' new position.

Although the overall dispersal process was the same for raccoons of all ages, there were slight differences between agents less than one year of age and all other agents. All agents less than one year old were subject to the dispersal process, whereas agents at least one year old only went through the dispersal process if they were occupying a cell above carrying capacity. The expected movement distance also varied based on age: the expected distance for agents less than 1 year of age was 0.75 grid cells, other agents had an expected distance of 0.5 grid cells. Because agents were subject to the dispersal process for a total of 4 weeks and could make multiple movements, this resulted in expected total distances of 3 grid cells (1.5 km) for agents less than 1 year of age and an expected distance of 2 grid cells (1 km) for other agents eligible for dispersal. These distances are consistent with empirical dispersal distances (Rees et al., 2008).

Disease initialization. We initialized the disease in week 1 of year 2 by randomly selecting 10 non-immune agents and changing their incubation state to 1.

Additional Literature Cited

Bastille-Rousseau, G., Gorman, N. T., McClure, K. M., Nituch, L., Buchanan, T., Chipman, R. B., Gilbert, A. T., & Pepin, K. M. (2024). Assessing the Efficiency of Local Rabies Vaccination Strategies for Raccoons (Procyon lotor) in an Urban Setting. *Journal of Wildlife Diseases*, *60*(1). https://doi.org/10.7589/JWD-D-23-00059

Beasley, E. M., Nelson, K. M., Slate, D., Gilbert, A. T., Pogmore, F. E., Chipman, R. B., & Davis, A. J. (2024). Oral Rabies Vaccination of Raccoons (Procyon lotor) across a Development Intensity Gradient in Burlington, Vermont, USA, 2015–2017. *Journal of Wildlife Diseases*, *60*(1), 1–13. https://doi.org/10.7589/JWD-D-22-00117

Bezanson, J., Edelman, A., Karpinski, S., & Shah, V. B. (2017). Julia: A fresh approach to numerical computing. *SIAM Review*, *59*(1), 65–98.

Cullingham, C. I., Pond, B. A., Kyle, C. J., Rees, E. E., Rosatte, R. C., & White, B. N. (2008). Combining direct and indirect genetic methods to estimate dispersal for informing wildlife disease management decisions. *Molecular Ecology*, *17*(22), 4874–4886. https://doi.org/10.1111/j.1365-294X.2008.03956.x

Etherington, T. R., Holland, E. P., & O'Sullivan, D. (2015). NLMpy: A python software package for the creation of neutral landscape models within a general numerical framework. *Methods in Ecology and Evolution*, *6*(2), 164–168. https://doi.org/10.1111/2041-210X.12308

Fehlner-Gardiner, C., Rudd, R., Donovan, D., Slate, D., Kempf, L., & Badcock, J. (2012). Comparing ONRAB And RABORAL V-RG oral rabies vaccine field performance in raccoons and striped skunks, New Brunswick, Canada, and Maine, USA. *Journal of Wildlife Diseases*, *48*(1), 157–167.

Fournier, A., Fussell, D., & Carpenter, L. (1982). Computer rendering of stochastic models. *Communications of the ACM*, *25*(6), 371–384. https://doi.org/10.1145/358523.358553

Fry, T. L., VanDalen, K. K., Shriner, S. A., Moore, S. M., Hanlon, C. A., & VerCauteren, K. C. (2013). Humoral immune response to oral rabies vaccination in raccoon kits: Problems and implications. *Vaccine*, *31*(26), 2811–2815. https://doi.org/10.1016/j.vaccine.2013.04.016

Grimm, V., Berger, U., Bastiansen, F., Eliassen, S., Ginot, V., Giske, J., Goss-Custard, J., Grand, T., Heinz, S. K., Huse, G., Huth, A., Jepsen, J. U., Jørgensen, C., Mooij, W. M., Müller, B., Pe'er, G., Piou, C., Railsback, S. F., Robbins, A. M., … DeAngelis, D. L. (2006). A standard protocol for describing individual-based and agent-based models. *Ecological Modelling*, *198*(1), 115–126. https://doi.org/10.1016/j.ecolmodel.2006.04.023

Grimm, V., Berger, U., DeAngelis, D. L., Polhill, J. G., Giske, J., & Railsback, S. F. (2010). The ODD protocol: A review and first update. *Ecological Modelling*, *221*(23), 2760–2768. https://doi.org/10.1016/j.ecolmodel.2010.08.019

Hesselbarth, M. H. K., Sciaini, M., With, K. A., Wiegand, K., & Nowosad, J. (2019). landscapemetrics: An open-source R tool to calculate landscape metrics. *Ecography*, *42*(10), 1648–1657. https://doi.org/10.1111/ecog.04617

Homer, C., Dewitz, J., Yang, L., Jin, S., Danielson, P., Xian, G., Coulston, J., Herold, N., Wickham, J., & Megown, K. (2015). Completion of the 2011 National Land Cover Database for the Conterminous United States – Representing a Decade of Land Cover Change Information. *Photogrammetric Engineering & Remote Sensing*, *81*(5), 345–354. https://doi.org/10.1016/S0099-1112(15)30100-2

Johnson, S. R., Slate, D., Nelson, K. M., Davis, A. J., Mills, S. A., Forbes, J. T., VerCauteren, K. C., Gilbert, A. T., & Chipman, R. B. (2021). Serological responses of raccoons and striped skunks to Ontario rabies vaccine bait in West Virginia during 2012–2016. *Viruses*, *13*(2), 157.

McClure, K. M., Bastille-Rousseau, G., Davis, A. J., Stengel, C. A., Nelson, K. M., Chipman, R. B., Wittemyer, G., Abdo, Z., Gilbert, A. T., & Pepin, K. M. (2022). Accounting for animal movement improves vaccination strategies against wildlife disease in heterogeneous landscapes. *Ecological Applications*, *32*(4), e2568.

Pitt, J. A., Larivière, S., & Messier, F. (2008). Survival and Body Condition of Raccoons at the Edge of the Range. *The Journal of Wildlife Management*, *72*(2), 389–395. https://doi.org/10.2193/2005-761

Prange, S., Gehrt, S. D., & Wiggers, E. P. (2004). Influences of anthropogenic resources on raccoon (Procyon lotor) movements and spatial distribution. *Journal of Mammalogy*, *85*(3), 483–490.

Rees, E. E., Pond, B. A., Phillips, J. R., & Murray, D. (2008). Raccoon ecology database: A resource for population dynamics modelling and meta-analysis. *Ecological Informatics*, *3*(1), 87–96. https://doi.org/10.1016/j.ecoinf.2008.01.002

Rees, E. E., Pond, B. A., Tinline, R. R., & Bélanger, D. (2013). Modelling the effect of landscape heterogeneity on the efficacy of vaccination for wildlife infectious disease control. *Journal of Applied Ecology*, *50*(4), 881–891. https://doi.org/10.1111/1365-2664.12101

Signer, J., Fieberg, J., & Avgar, T. (2017). Estimating utilization distributions from fitted step-selection functions. *Ecosphere*, *8*(4), e01771. https://doi.org/10.1002/ecs2.1771

Tinline, R., Ball, D., Broadfoot, J., & Pond, B. (2007). The Ontario rabies model. *Queens University, Kingston, Ontario, Canada*.

Appendix 2: Model Functionality Testing and Parameter Sensitivity Analysis

We tested various aspects of the agent-based model (see Appendix 1 for detailed descriptions of individual functions) to ensure they were producing expected outputs. For most model parameters, we assigned values based on empirical data, but for parameters for which empirical values were limited, we conducted a parameter sensitivity analysis to identify values that produced realistic outcomes. Results of both tests are discussed below. Unless otherwise indicated, functionality tests and parameter sensitivity analyses were completed without agents immigrating into the landscape.

Functionality Tests

Cell Size

We chose a 0.5 x 0.5 km cell for our spatial grain size. This grain size reduces computational intensity compared to a smaller grain size (e.g. the 30 x 30 m resolution of the available land cover data). Additionally, there is little habitat heterogeneity at the 30 x 30 m resolution in the greater Burlington area, the empirical landscape from which we derived the characteristics of our simulated landscapes. As a result, the autocorrelation of the original 30 x 30 m landscape calculated using the package `landscapemetrics` (Hesselbarth et al., 2019) was similar to the landscape with a 0.5 x 0.5 km resolution (75.8 vs. 77.4, respectively). The major features in a map of Burlington at a 30 x 30 m resolution were still present in a map with a 0.5 x 0.5 km resolution (Figure 2-1).

We decided against using a larger grain size than 0.5 x 0.5 km because 1) the major landscape features are less identifiable at larger grain sizes, and 2) increasing the grain size would restrict agents' home ranges to approximately 1 cell or less, which would prevent agents from readily changing their weekly position.

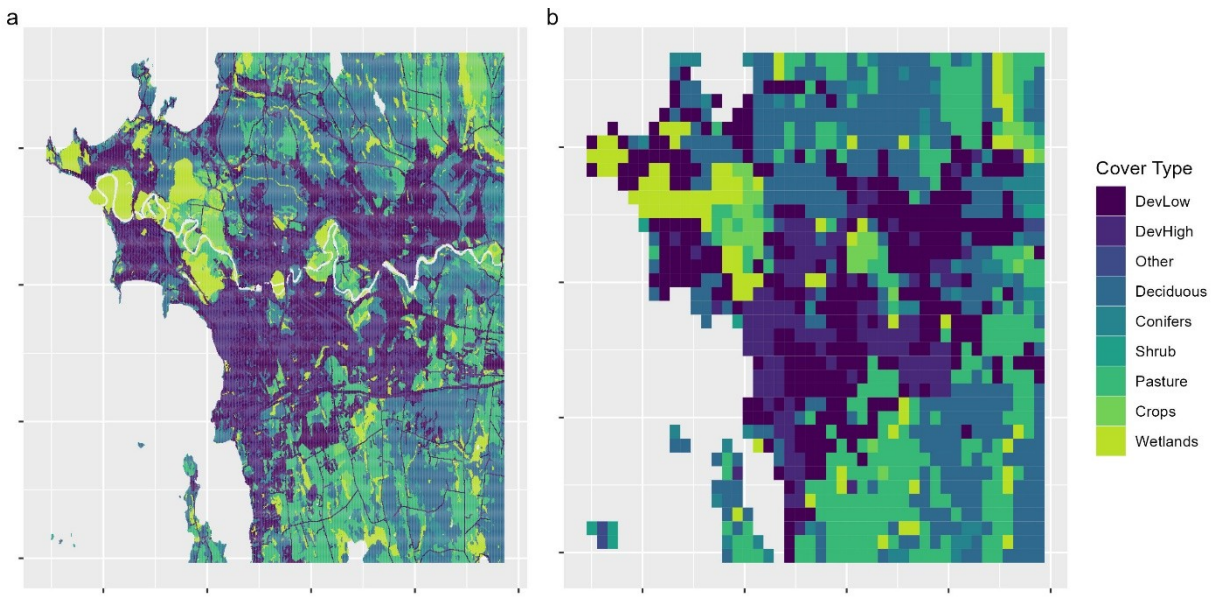

Figure 2-1. Map of the greater Burlington, VT area at a 30 x 30 m resolution (a) and 0.5 x 0.5 km resolution (b). Due to a high degree of spatial autocorrelation in land cover, major landmarks, including the wetlands of the Winooski River delta and Intervale Center farmland in the top-left corner, and the municipalities of Burlington, South Burlington, Winooski, and Essex Junction in the center, are still recognizable with the larger spatial grain.

Landscape Generation Algorithm

We used the midpoint displacement algorithm in the Julia package `NeutralLandscapes` (Poisot et al., 2023), which is a port of the Python package `NLMpy` (Etherington et al., 2015), to generate our simulated landscapes. This algorithm simulates a landscape of values of a continuous variable such as elevation, the autocorrelation of which is specified by the user (Fournier et al., 1982; Palmer, 1992). We calculated the spatial autocorrelation of Burlington habitat data using `lsm_l_ai` function in the R package `landscapemetrics` (Hesselbarth et al., 2019) and used that value in the mid-point displacement algorithm. After generating a continuous landscape using the mid-point displacement algorithm, we re-classified the simulated landscape into discrete categories based on the

relative proportions of available habitat in Burlington (Figure 2-2). We also placed a unique "buffer" habitat on the outermost 5 cells on each side of the simulated landscape, which were used to reduce boundary effects in the simulation (see Appendix 1 for more details).

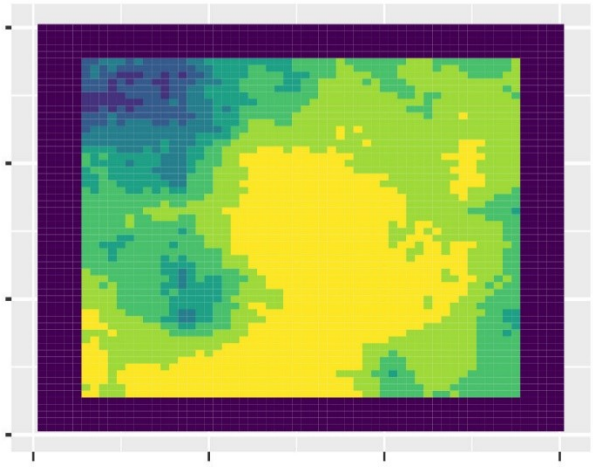

Figure 2-2. Example landscape generated using a mid-point displacement algorithm and re-classified into discrete habitat categories. Spatial autocorrelation and relative proportions of land cover categories were calculated from land cover data of the greater Burlington, VT area.

Weekly Position and Seasonal Home Range

Each agent was assigned a weekly position at each time step in the simulation, which represented the center of the agent's weekly home range. In addition, each agent was assigned a home range attractor that restricted the agent's movement to a particular geographic area. The home range attractor could be updated annually during the dispersal period. The weekly position was updated each week based on a weighted probability that accounted for 1) the habitat type, 2) conspecific density, and 3) distance from the agent's home range attractor in the agent's current weekly position and the 8 cells

surrounding its weekly position. For more details, see the *Movement* subsection of Appendix 1, Section VII: Submodels.

We tested the movement of agents prior to the dispersal period of the model to ensure seasonal home range size was consistent with empirical values from Burlington. Because empirical data from Burlington spans from July–September, we calculated agents' seasonal home ranges from the equivalent weeks of the simulation. A distance-decay rate from the home range attractor of -0.1 resulted in seasonal home ranges that ranged from 0.196–3.298 km^2 in size, with a mean value of 1.121 km^2. The mean home range size was very close to the estimated empirical average of approximately 1.13 km^2 in Burlington (McClure et al., 2022). Variability in home range sizes can affect rabies persistence (McClure et al., 2020), but because we were primarily interested in the affects of immigration on rabies persistence and recolonization, we chose not to introduce additional variability in seasonal home range size.

Disease State Changes

Rabies typically has a latent period of 3–6 weeks, in which an individual has been infected with the virus but is not yet contagious (Tinline et al., 2007). We modeled the weekly probability of an agent moving from the "exposed" (i.e. infected but not contagious) to the "infectious" (i.e. contagious) state as the outcome of a Bernoulli trial, in which the probability of changing states was drawn from a beta distribution $P \sim Beta(n, 5)$, where n is the number of weeks the agent has spent in the exposed state. This resulted in a typical latent period of 3–6 weeks, which is consistent with empirical values (Figure 2-3).

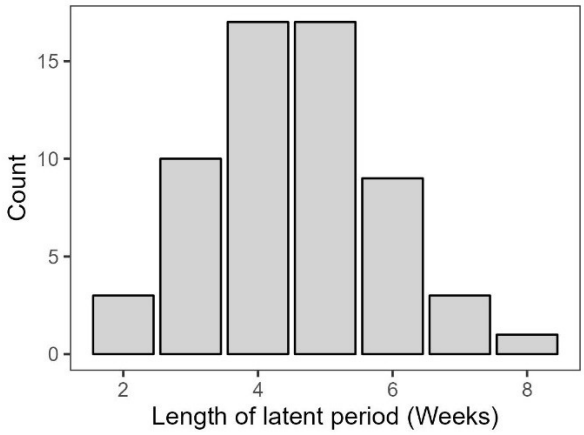

Figure 2-3. Distribution of the length of the latent period of the disease, in weeks. The distribution has a mode of 4–5 weeks; consistent with empirical values.

Raccoons exposed to the rabies virus also have a 10% probability of recovering from the virus rather than becoming infectious (Slate et al., 2014). We modeled the weekly process of an exposed individual entering the recovered state as the outcome of a Bernoulli trial, in which the probability of success was 0.015, resulting in simulated recovery rates ranging from 8–12%.

Parameter Sensitivity Analyses

K_{max} and Carrying Capacity Mortality

Empirical data from Burlington suggests a mean raccoon density of approximately 15/km^2 in July and 11/km^2 in October (Beasley et al., 2024). We tested the sensitivity of all possible combinations of maximum grid cell capacity (K_{max}) and two different mortality rates that were applied to grid cells in which the number of raccoons exceeded K_{max} in a given week. We tested different mortality rates for raccoons greater than 1 year of age ("adults") and raccoons 1 year of age or less ("juveniles") to represent the higher juvenile mortality rates seen in empirical data(Pitt et al., 2008) We completed 20 replicates of each possible combination of K_{max}, adult carrying capacity mortality, and juvenile carrying capacity mortality (Table 2-1).

Of the parameter combinations tested, seven combinations yielded summer and fall raccoon densities that were reasonably close to empirical values (Figure 2-4). Of these, the empirical densities fell within the 25–75% quantile of three combinations of parameters (Figures 2-4, 2-5). All three parameter combinations also resulted in a population that was slowly growing. We ultimately chose a K_{max} of 30, adult mortality rate of 0.0075, and juvenile mortality rate of 0.015 because this combination resulted in a less variable population size (Figure 2-5), reducing the amount of noise in the results.

Table 2-1. Parameters and values tested for the parameter sensitivity analyses.

Parameter	**Values tested**
Carrying capacity per cell (K_{max})	20, 25, 30
Carrying capacity mortality (> 52 weeks of age)	0.005, 0.0075, 0.01
Carrying capacity mortality (<= 52 weeks of age)	0.015, 0.02, 0.025
λ_1	0.01, 0.015, 0.02, 0.025, 0.03
λ_2	0.004, 0.005, 0.006, 0.007
Starting number of cases	5, 10, 20, 40
Landscape size	40x40, 60x60, 80x80, 100x100

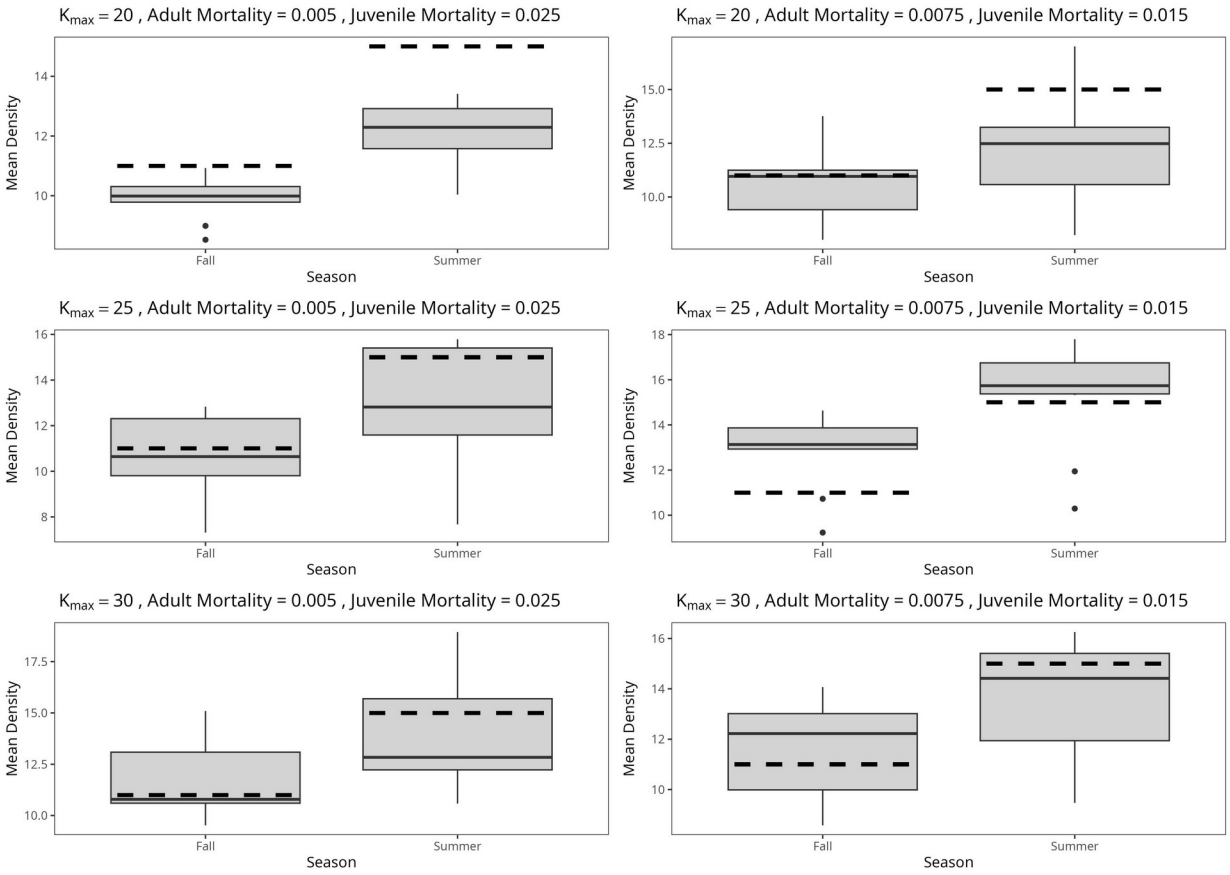

Figure 2-4. Simulated mean raccoon densities (raccoons per km^2) in the fall and summer for various combinations of grid-cell carrying capacity (K_{max}) and carrying capacity-related mortality rates for adult and juvenile raccoons. Horizontal dashed lines represent approximate raccoon densities based on empirical data.

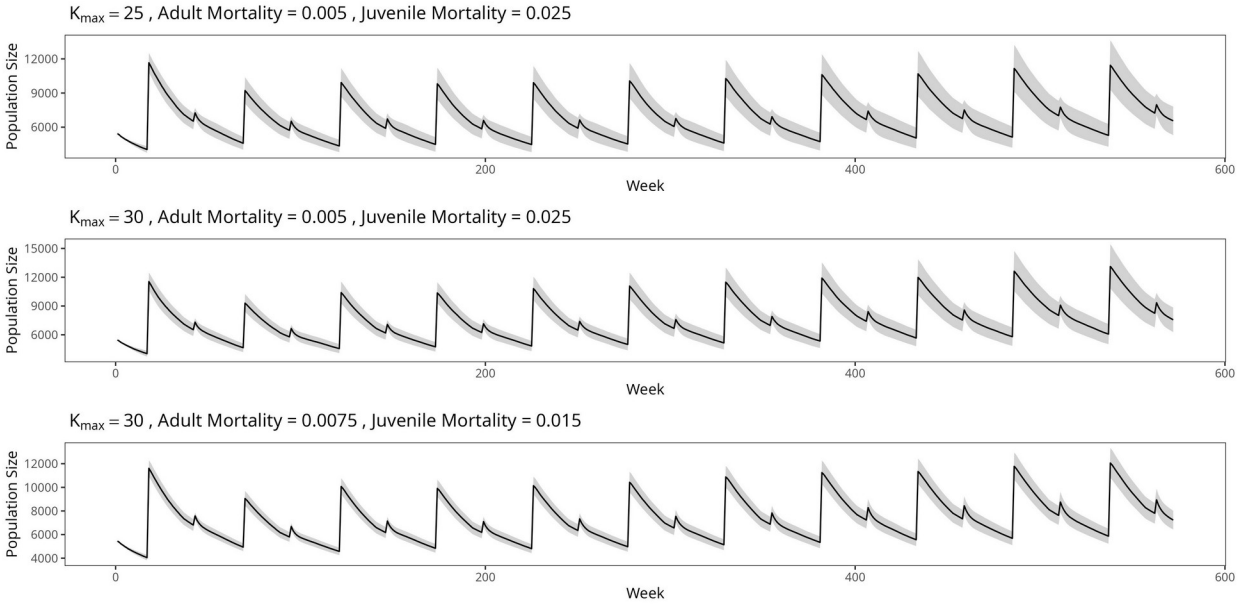

Figure 2-5. Simulated raccoon population sizes across an 11-year simulation at various combinations of parameter values. Black lines denote the mean population size across replicates and gray shading denotes the 95% confidence interval. Although all of the above parameter combinations yielded realistic raccoon densities (Figure 2-4) and populations that were slowly growing, a grid-cell carrying capacity (K_{max}) of 30, an adult carrying capacity-induced mortality rate of 0.0075, and a juvenile carrying capacity-induced mortality rate of 0.015 (bottom panel) were ultimately chosen because this combination yielded the least variability across replicates.

Disease Transmission Rates

We tested several combinations of values of core home range (λ_1, corresponding to the transmission rate to raccoons within 0.5 km of the infectious raccoon) and peripheral home range (λ_2, corresponding to transmission to raccoons within 1 km of the infectious agent) transmission rates in simulations with the density mortality rates discussed above. We tuned the core home range transmission rate first by performing a wide sweep of parameter values between 0.001 and 0.5 on a logarithmic scale, with 10 replicates per parameter value. We dropped transmission rates in which rabies was eliminated in 100% of simulations. Of these, transmission rates of 0.0224 and 0.0349

resulted in simulations in which rabies was elimated in 45% of simulations, typically persisted into year 7 of the simulation when it was elminated (week 364, Figure 2-6), and an effective reproduction number R_e close to the empirical value of 1.13 (Biek et al., 2007; Childs et al., 2000; Figure 2-8).

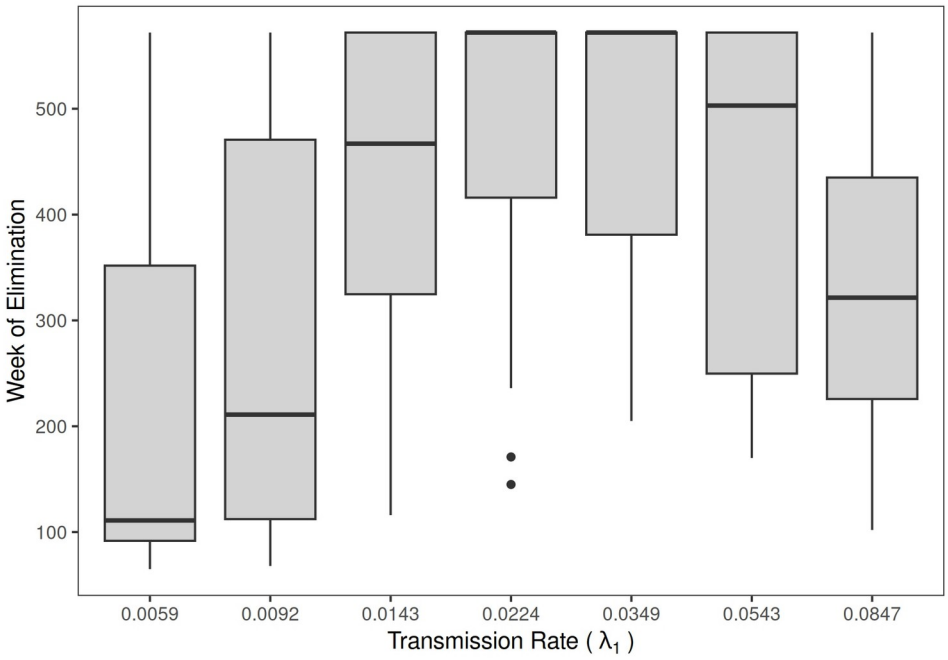

Figure 2-6. Median week of elimination across simulations with varying core home range rabies transmission rates. Transmission rates between 0.0143 and 0.0543 typically resulted in simulations where rabies persisted beyond year 7 (week 364).

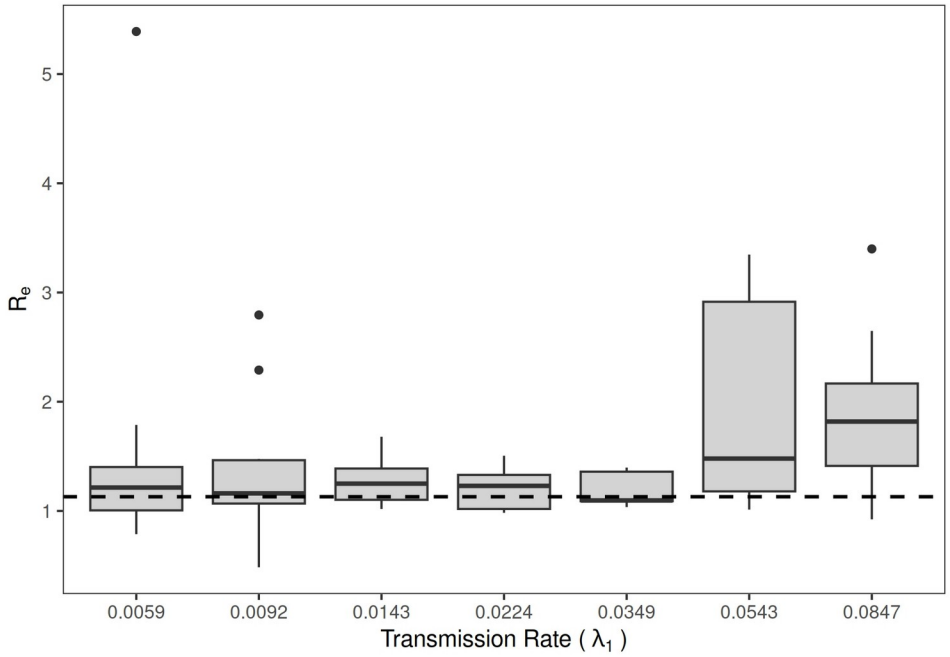

Figure 2-8. Effective reproduction number (R_e) across simulations with varying core home range rabies transmission rates. Transmission rates less than 0.05 typically yielded simulations with an R_e close to the empirical value of 1.13 (dashed line).

We then tested a series of values for transmission rates at the periphery of an infected agent's weekly home range λ_2 (i.e. within 1 km of the agent's current position). We began with a logarithmic sequence of values ranging from 0.001–0.03, with 10 replicates per value and λ_1 fixed at 0.0275 (approximate midpoint between the values selected in the broad sweep of λ_1 values). Rabies elimination ranged from 30–70%, with no clear associations with λ_2 values. There was no clear association between λ_2 and elimination time (Figure 2-9). Median weekly cases also varied, but were typically approximately 8 cases per week (Figure 2-10). Most values of λ_2 yielded R_e values that were slightly too high, typically ranging from 1.2–1.4; although the 75% quantiles for each value of λ_2 encompassed the empirical R_e of 1.13 (Figure 2-11).

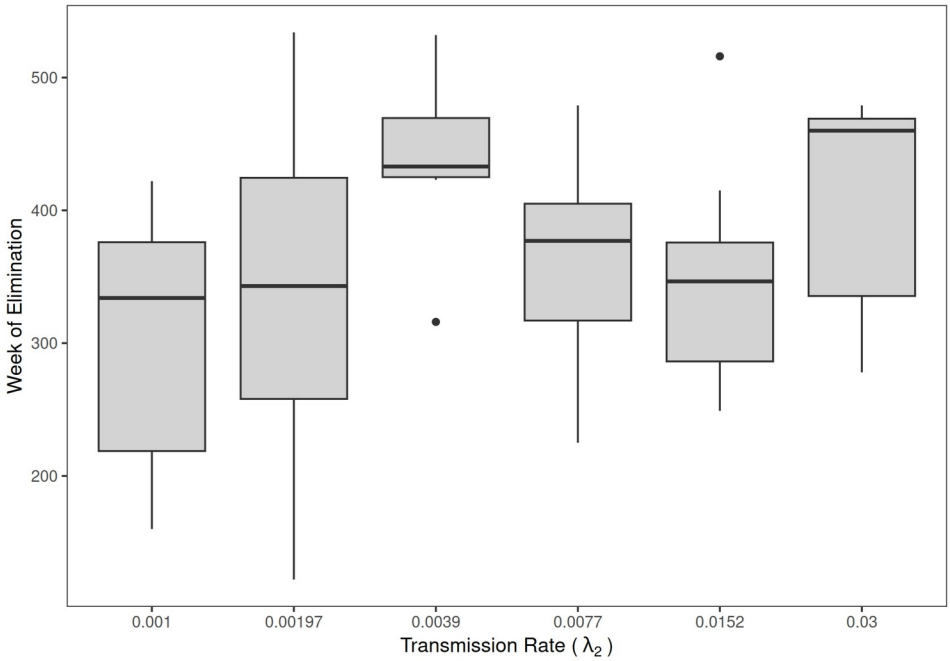

Figure 2-9. Median week of elimination across simulations with varying peripheral home range rabies transmission rates. Transmission rates of 0.0039 typically resulted in simulations where rabies persisted beyond year 8 (week 416).

Based on the results of the broad sweep of λ values, we chose to further test λ_1 values from 0.015–0.035 at intervals of 0.5, and λ_2 values of 0.002–0.005 at intervals of 0.001.

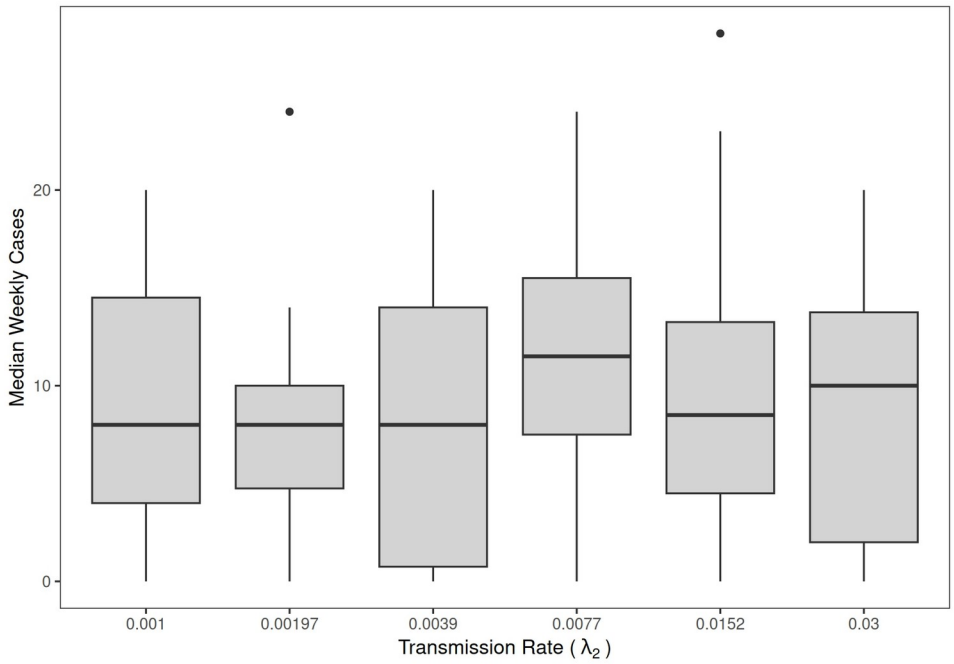

Figure 2-10. Median weekly cases across simulations with varying peripheral home range rabies transmission rates. Most transmission rates typically resulted in fewer than 10 cases per week; the exceptions being 0.0077 and 0.03.

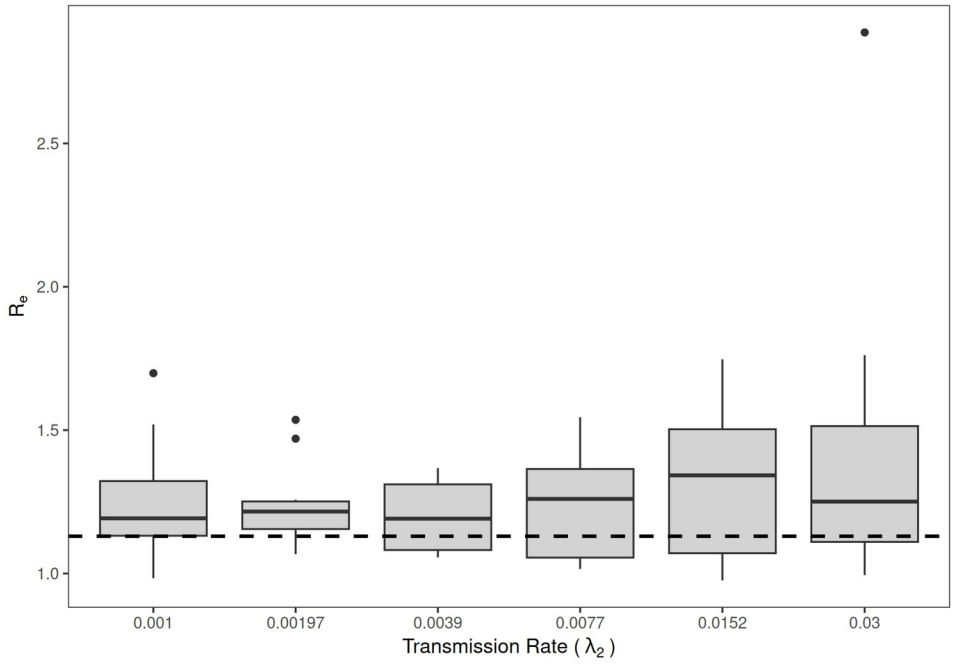

Figure 2-11. Effective reproduction number (R_e) across simulations with varying peripheral home range rabies transmission rates. Transmission rates greater than 0.001 typically yielded R_e values ranging from 1.2–1.4, which is slightly higher than empirical values (dashed line).

Lastly, we completed a parameter sweep testing all combinations of λ_1 ranging from 0.015–0.035 at intervals of 0.005, and λ_2 from 0.002–0.005 at intervals of 0.001, with 20 replicates per combination. Elimination probabilities ranged from 0.3–0.7 with no clear association between elimination probability and transmission rate. Landscapes typically reached elimination more rapidly in landscapes with low values of λ_1 and high values of λ_2 (Figure 2-12). Median weekly cases typically ranged from 5–11 cases, with the highest numbers of median cases typically occurring when both transmission probabilities were relatively high (Figure 2-13). Effective reproduction number R_e values ranged from 1.1–1.5, with no clear pattern across the tested range of transmission rates (Figure 2-14).

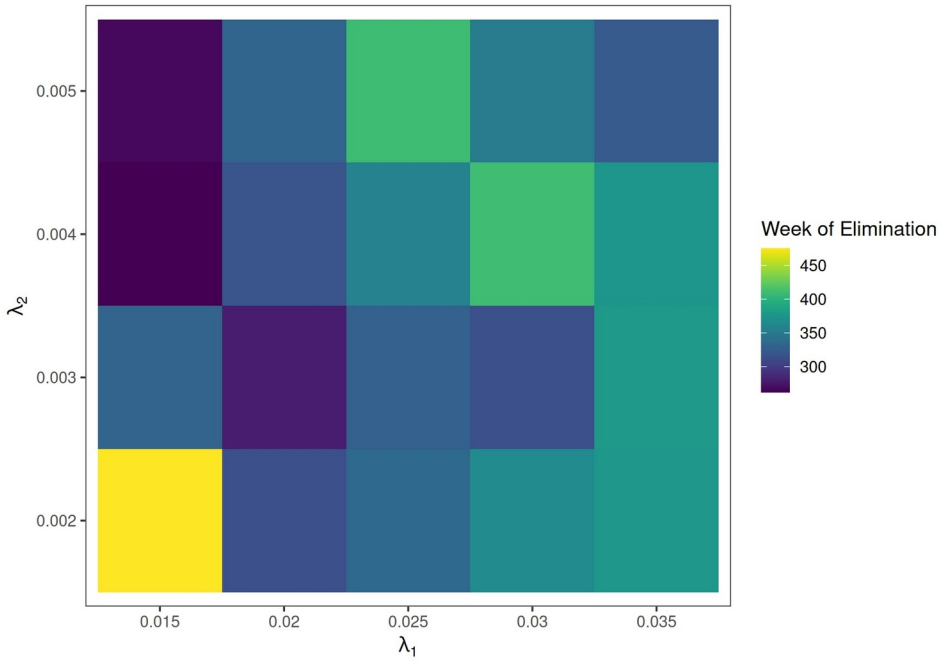

Figure 2-12. Median time, in weeks, rabies elimination in simulated landscapes across various combinations of within-cell (λ_1) and between-cell (λ_2) transmission rates. Rabies was typically eliminated more quickly in landscapes with low λ_1 values and high λ_2 values.

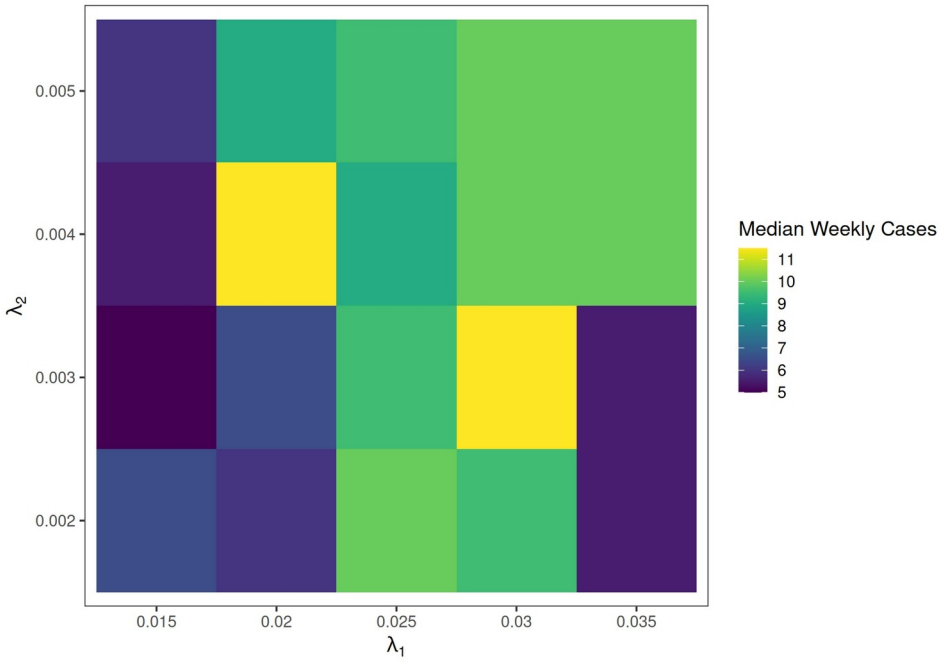

Figure 2-13. Median weekly cases across various combinations of within-cell (λ_1) and between-cell (λ_2) transmission rates. Most simulated landscapes had 10 or fewer weekly cases; weekly cases were generally higher when both transmission rates were high.

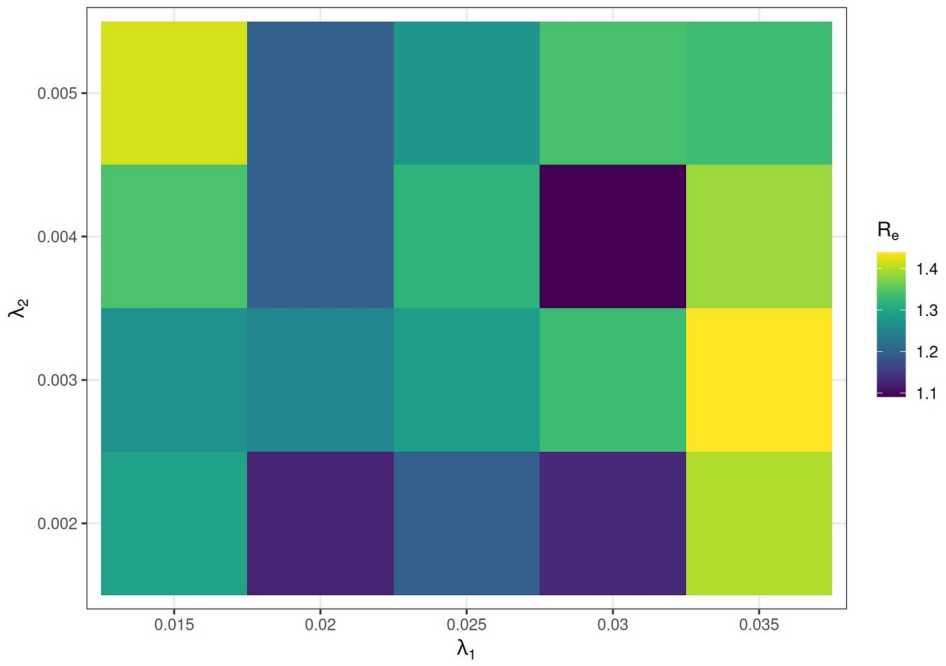

Figure 2-14. Effective reproductive rate (R_e) across various combinations of within-cell (λ_1) and between-cell (λ_2) transmission rates. Values of R_e ranged from 1.1–1.5, with most ranging from 1.2–1.4. Empirical estimates of R_e are approximately 1.13, which is lower than most simulated values.

Two parameter combinations yielded realistic outcomes of 1) rabies persistence for a median of 7 years, 2) fewer than 10 cases per week, and 3) median R_e values between 1.1 and 1.3. We chose a λ_1 of 0.025 and a λ_2 of 0.005 because this combination resulted in a small, though still noticeable, decrease in population size after the disease is introduced and a population that grows slowly (Figure 2-15), which is thought to occur in real populations.

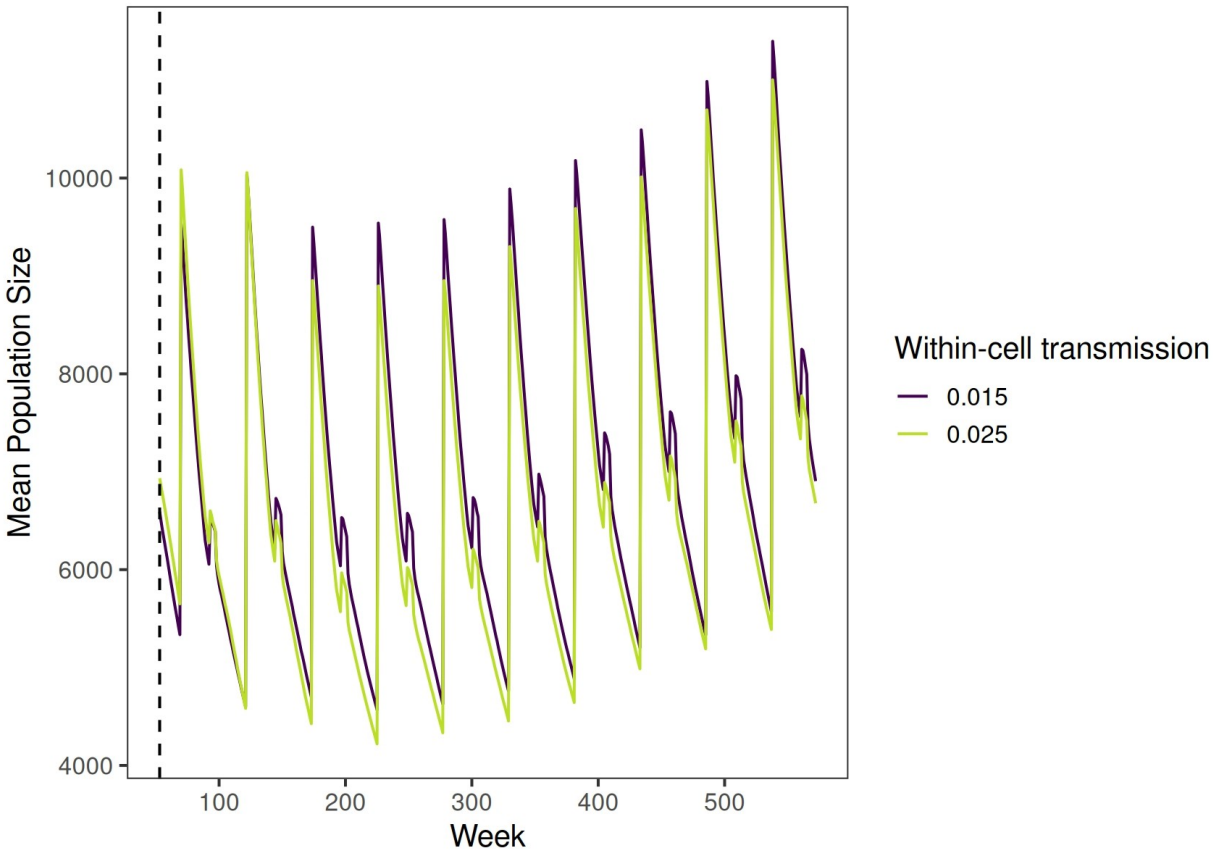

Figure 2-15. Median population size per week of the simulation combinations of within-cell (λ_1) and between-cell (λ_2) transmission rates which were already filtered for realistic outcomes. Real populations are thought to experience a small population decrease after rabies is introduced (dashed vertical line), followed by a slow increase as the initial wave of cases passes.

Disease Starting Cases

We tested the effects of the number of starting cases on rabies elimination probability and time, median and maximum weekly cases, and the effective reproductive rate R_e. We completed simulations with 5, 10, 20, and 40 starting cases, with 20 replicates each and transmission rates fixed as above. Elimination probability ranged from 45–55% with no clear association with the number of starting cases. The number of starting cases had no clear effect on median weekly cases (Figure 2-16). Time to

elimination (Figure 2-17) and R_e (Figure 2-18) may increase slightly with increasing numbers of starting cases; however, due to high variability the effect is not clear. The number of starting cases had a clear effect on maximum weekly cases: simulations with 20 and 40 starting cases had an observably higher maximum than simulations with 5 or 10 starting cases (Figure 2-19). The timing of peak cases also varied with the number of starting cases, occurring earlier in the simulation as starting cases increased (Figure 2-20).

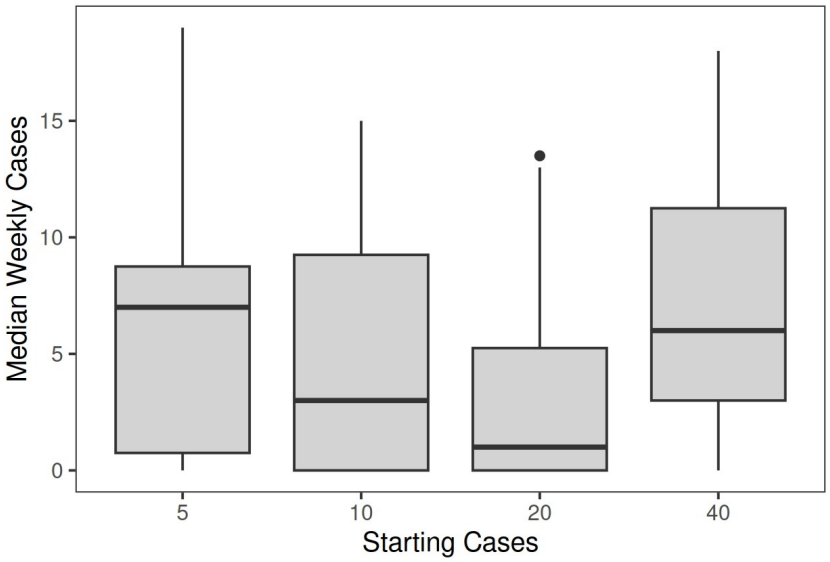

Figure 2-16. Median weekly cases across simulations with varying numbers of starting cases used to initialize the disease. There is no clear association between median weekly cases and the number of starting cases.

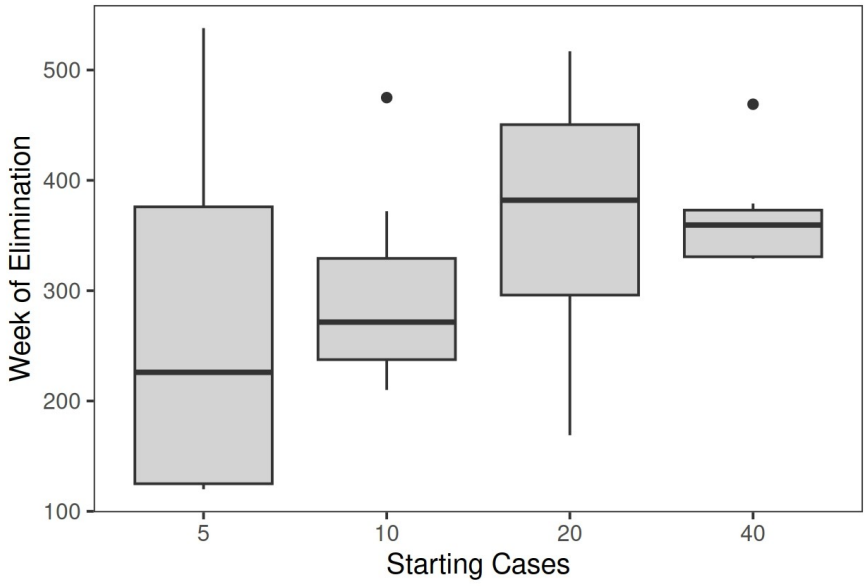

Figure 2-17. Median weeks until rabies elimination across simulations with varying numbers of starting cases used to initialize the disease. Time to elimination appears to increase with the number of starting cases; however, due to high variability in simulations with 5 and 20 starting cases, this association is unclear.

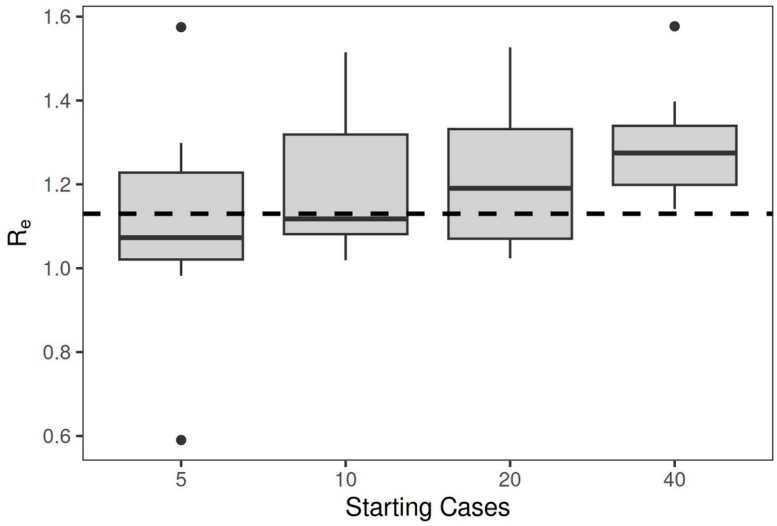

Figure 2-18. Effective reproductive rate R_e across simulations with varying numbers of starting cases used to initialize the disease. Increasing starting cases appears to result in a slight increase in R_e; however, due to the high degree of overlap between simulations with varying starting cases, this

association is unclear. The 75% quartiles of simulations with 5, 10, and 20 cases overlapped with the empirical R_e of 1.13 (dashed line).

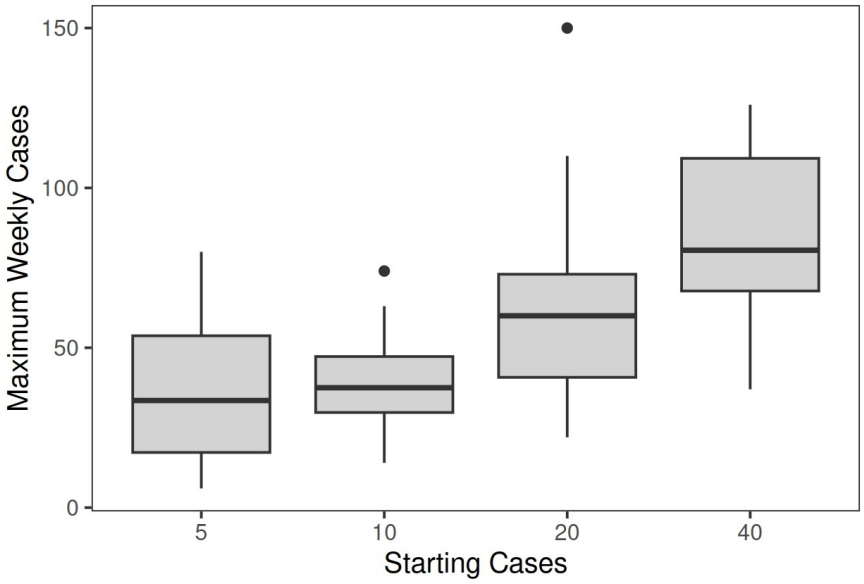

Figure 2-19. Maximum weekly cases across simulations with varying numbers of starting cases used to initialize the disease. Increasing the number of starting cases resulted in increased maximum weekly cases in simulations with more than 10 starting cases.

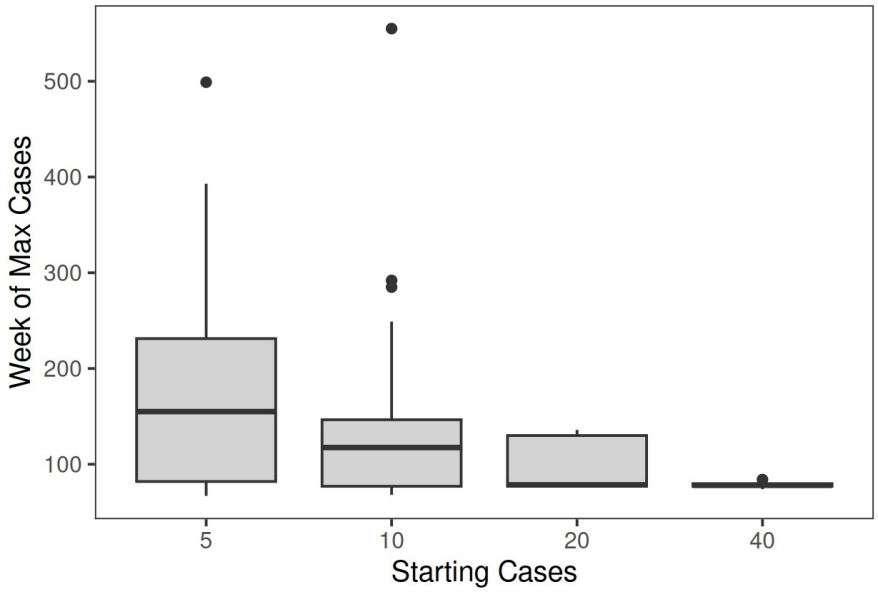

Figure 2-20. Timing of maximum weekly cases across simulations with varying numbers of starting cases used to initialize the disease. Increasing the number of starting cases resulted in a maximum that occurred earlier in the simulation, with lower variability in the timing of the maximum.

We ultimately chose 10 starting cases due to 1) a median R_e value that is closest to the empirical value, 2) a smaller number of maximum weekly cases compared to simulations with higher numbers of starting cases, and 3) more variability in the timing of the case peak compared to simulations with higher numbers of starting cases.

Population turnover

Because population turnover (i.e. births vs. deaths) affects the relative proportion of susceptible to recovered/vaccinated individuals in the population, we assessed whether the above values of carrying capacity- and disease-related parameters yielded realistic rates of turnover. We simulated 2 years of the population: one without the disease, and one following disease introduction on week 1 of year 2. The annual birth pulse approximately doubled the population during the week in which births

occurred. However, year-over-year population growth with the density mortality rates described above ranged from -1.58%–1.79%, with a median growth rate of 1.29%.

Weekly deaths ranged from 0.6–7.5% of the population, with a median of 1.4%. Prior to disease introduction, mortality rates were highest between weeks 20 and 40 of the simulation (Figure 2-21) due to high carrying capacity-induced mortality of agents less than 52 weeks of age, which ranged from 20–100% of deaths with a median of 61.5% of deaths during this time period. This is qualitatively consistent with higher juvenile mortality rates in natural populations (Pitt et al., 2008). Over the course of a year, carrying capacity-induced mortality of agents was the most common source of mortality (74.0% of all mortality events before disease introduction).

After the disease was introduced into the population, mortality rates tended to be higher earlier in the year, although this could be an artifact of disease introduction, as mortality rates with and without the disease were similar at the end of the year (Figure 2-21). The most common source of mortality post-disease introduction was still carrying capacity mortality of agents less than 52 weeks of age, accounting for 40.5% of deaths over the course of the year. Disease-induced mortality accounted for 35.2% of deaths, while carrying capacity mortality of agents over 52 weeks of age accounted for 13.9% of deaths.

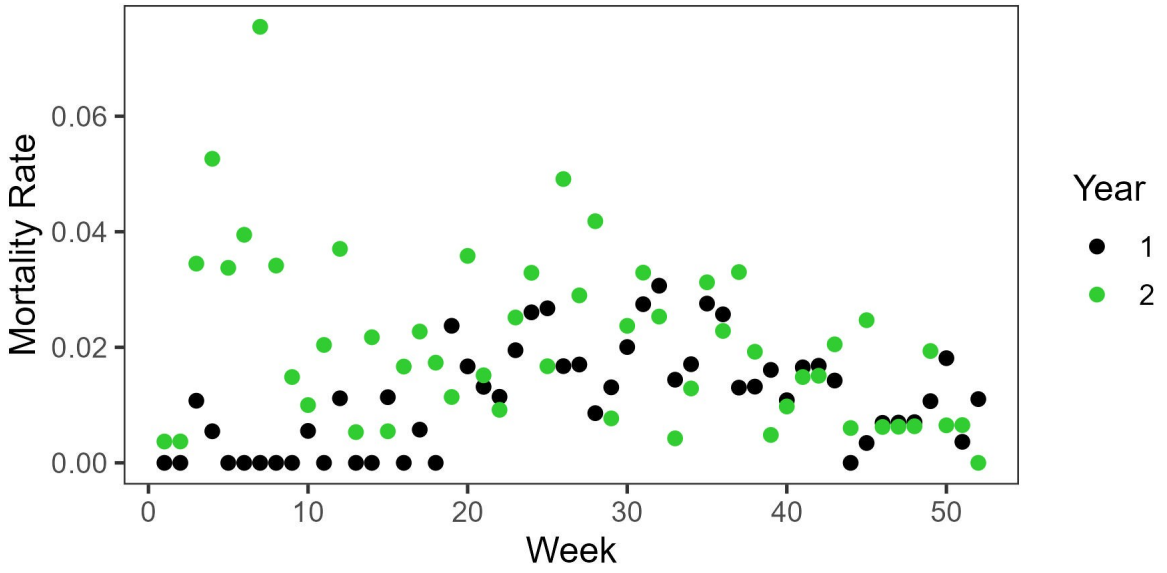

Figure 2-21. Weekly mortality rates before (black) and after (green) rabies was introduced into the simulated population. Mortality rates were generally low, with a median rate of 0.014. Prior to disease introduction, mortality rates were highest between weeks 20 and 40 of the simulation, a time period after the birth of new agents but before the dispersal period. After disease introduction, mortality rates were slightly higher earlier in the year, although this could be an artifact of disease initialization.

Landscape Size

We tested the effect of landscape size on rabies elimination and median prevalence by simulating 20 replicates each of landscapes with a 40x40, 60x60, 80x80, and 100x100 cell grid. Elimination probability decreased with landscape size: elimination was reached in 80% of 40x40 landscapes, 65% of 60x60 landscapes, and 5% of 80x80 and 100x100 landscapes. Rabies prevalence did not differ between simulations with different landscape sizes (Figure 2-22).

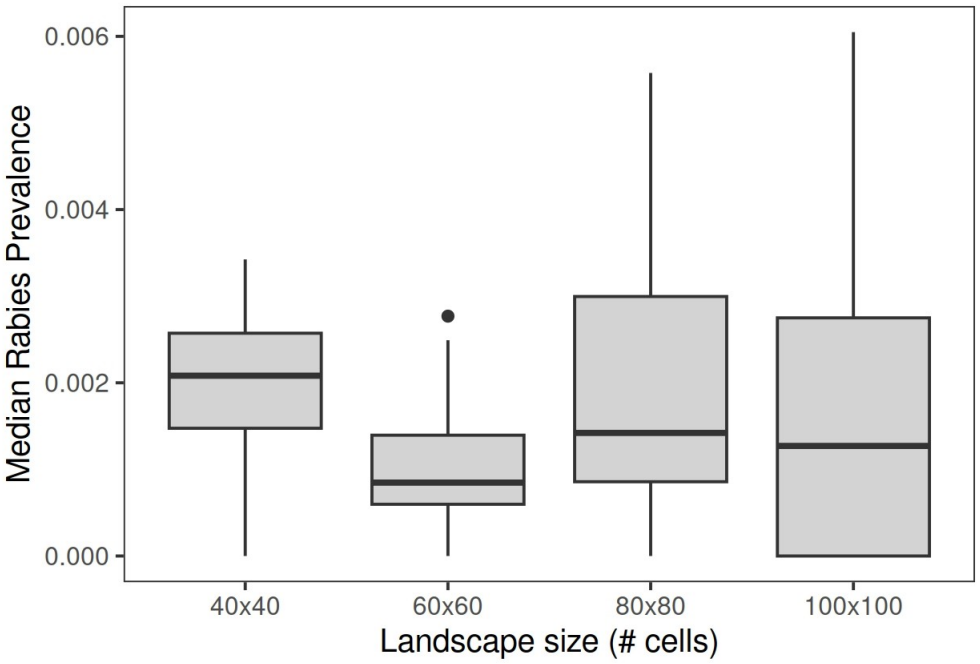

Figure 2-22. Median rabies prevalence across simulated landscapes of varying sizes. Prevalence was only calculated from time steps in which rabies still persisted in the landscape. Rabies prevalence did not clearly differ among landscapes of different sizes.

Table of Parameters

Values for demographic and epidemiological parameters can be found in the following table (Table 2-2).

Table 2-2. Parameter values for demographic and epidemiological parameters from the agent-based model.

Parameter	Value(s)	Description and Source
Raccoon demographics		
K_{max}	30	Maximum carrying capacity per cell (Figures 2-4, 2-5)
Age of independence	20 weeks	Age at which juveniles are no longer maternally dependent: can survive if mother dies & moves independently, but still shares a home range attractor

		(Rees et al., 2008; Tinline et al., 2007)
Week of birth	Week 18	(Hauver et al., 2010; Rees et al., 2008; Sanderson & Nalbandov, 1973)
Probability of a female > 52 weeks old producing a litter	95%	(Prange et al., 2003)
Litter size	~ Pois(4)	(Rees et al., 2008)
Dispersal timing	Weeks 41–45	Adults only disperse if their current position exceeds carrying capacity (Rees et al., 2008)
Dispersal distance	~Pois(0.75) (< 52 weeks of age) ~Pois(0.5) (>= 52 weeks of age)	For ~Pois(λ) in which λ represents the expected number of 0.5 km x 0.5 km grid cells moved. Eligible agents undergo the Poisson trial 4 times in weeks 41–45 (Rees et al., 2008)
Weekly stochastic mortality	0.001	Represents all sources of mortality not explicitly defined here (Gehrt & Prange, 2007; Prange et al., 2003)
Orphan mortality	100%	Applied to raccoons < 20 weeks of age whose mother is dead
Old age mortality	100%	Applied to raccoons over 8 years old (Rees et al., 2013)
Weekly density-related mortality rate	0.0075 (> 52 weeks) 0.015 (<= 52 weeks)	Applied to raccoons occupying cells exceeding K_{max} (Figures 2-4, 2-5)
Immigration Timing	Variable	Immigration occurs weekly ("consistent") or between weeks 40 and 50 ("seasonal")
Immigration Rate	~Pois(λ)	Variable. For consistent immigration, λ is set by the user (values of 1–5); for seasonal immigration, the number of immigrants is ~Pois(λ*5), resulting in approximately the same number of annual immigrants per value of λ.
Epidemiological parameters		
Probability of becoming infectious	*~Beta(n, 5)*	Where n = number of weeks since exposure. Results in a typical latent period of 3–6 weeks (Figure 2-3, Tinline et al., 2002)

Probability of recovery from exposure	0.002/week	Results in a total recovery rate of approximately 10% (Slate et al., 2014)
Infectious period	1 week	(Hanlon et al., 2007)
Transmission coefficient	$\lambda_1 = 0.02$ $\lambda_2 = 0.006$	In which λ_1 = transmission rate to raccoons occupying the same cell as the infected raccoon; λ_2 = transmission rate to raccoons occupying any other cell within the infected raccoon's home range (Figures 2-6 – 2-15)
Initial infection time	Year 2, Week 1	
Initial infections	10	Raccoons to be infected initially are randomly selected from non-immune raccoons (Figures 2-16 – 2-20)
Vaccination probability (raccoons at least 52 weeks of age)	Varies	Takes values from 0–80% at intervals of 10%
Vaccination probability (raccoons less than 52 weeks of age)	Vaccination probability / 2	(Beasley et al., 2024)
Immunity duration	Permanent	Vaccine-induced immunity duration is unknown. Previous work has included permanent immunity (e.g. McClure et al., 2020, but see Acheson et al., 2023)
Infection rate of immigrants	Varies	Values include 0, 0.015, 0.03, 0.045, and 0.06

Additional Literature Cited

Acheson, E. S., Viard, F., Buchanan, T., Nituch, L., & Leighton, P. A. (2023). Comparing Control Intervention Scenarios for Raccoon Rabies in Southern Ontario between 2015 and 2025. *Viruses*, *15*(2), Article 2. https://doi.org/10.3390/v15020528

Beasley, E. M., Nelson, K. M., Slate, D., Gilbert, A. T., Pogmore, F. E., Chipman, R. B., & Davis, A. J. (2024). Oral Rabies Vaccination of Raccoons (Procyon lotor) across a Development Intensity Gradient in Burlington, Vermont, USA, 2015–2017. *Journal of Wildlife Diseases*, *60*(1), 1–13. https://doi.org/10.7589/JWD-D-22-00117

Biek, R., Henderson, J. C., Waller, L. A., Rupprecht, C. E., & Real, L. A. (2007). A high-resolution genetic signature of demographic and spatial expansion in epizootic rabies virus. *Proceedings of the National Academy of Sciences*, *104*(19), 7993–7998. https://doi.org/10.1073/pnas.0700741104

Childs, J. E., Curns, A. T., Dey, M. E., Real, L. A., Feinstein, L., Bjørnstad, O. N., & Krebs, J. W. (2000). Predicting the local dynamics of epizootic rabies among raccoons in the United States. *Proceedings of the National Academy of Sciences*, *97*(25), 13666–13671. https://doi.org/10.1073/pnas.240326697

Etherington, T. R., Holland, E. P., & O'Sullivan, D. (2015). NLMpy: A python software package for the creation of neutral landscape models within a general numerical framework. *Methods in Ecology and Evolution*, *6*(2), 164–168. https://doi.org/10.1111/2041-210X.12308

Fournier, A., Fussell, D., & Carpenter, L. (1982). Computer rendering of stochastic models. *Communications of the ACM*, *25*(6), 371–384. https://doi.org/10.1145/358523.358553

Gehrt, S. D., & Prange, S. (2007). Interference competition between coyotes and raccoons: A test of the mesopredator release hypothesis. *Behavioral Ecology*, *18*(1), 204–214. https://doi.org/10.1093/beheco/arl075

Gross, J., Elvinger, F., Hungerford, L. L., & Gehrt, S. D. (2012). Raccoon use of the urban matrix in the Baltimore Metropolitan Area, Maryland. *Urban Ecosystems*, *15*(3), 667–682. https://doi.org/10.1007/s11252-011-0218-z

Hanlon, C. A., Niezgoda, M., & Rupprecht, C. E. (2007). 5—Rabies in Terrestrial Animals. In A. C. Jackson & W. H. Wunner (Eds.), *Rabies (Second Edition)* (pp. 201–258). Academic Press. https://doi.org/10.1016/B978-012369366-2/50007-5

Hauver, S. A., Gehrt, S. D., Prange, S., & Dubach, J. (2010). Behavioral and genetic aspects of the raccoon mating system. *Journal of Mammalogy*, *91*(3), 749–757. https://doi.org/10.1644/09-MAMM-A-067.1

Hesselbarth, M. H. K., Sciaini, M., With, K. A., Wiegand, K., & Nowosad, J. (2019). landscapemetrics: An open-source R tool to calculate landscape metrics. *Ecography*, *42*(10), 1648–1657. https://doi.org/10.1111/ecog.04617

McClure, K. M., Bastille-Rousseau, G., Davis, A. J., Stengel, C. A., Nelson, K. M., Chipman, R. B., Wittemyer, G., Abdo, Z., Gilbert, A. T., & Pepin, K. M. (2022). Accounting for animal movement improves vaccination strategies against wildlife disease in heterogeneous landscapes. *Ecological Applications*, *32*(4), e2568.

McClure, K. M., Gilbert, A. T., Chipman, R. B., Rees, E. E., & Pepin, K. M. (2020). Variation in host home range size decreases rabies vaccination effectiveness by increasing the spatial spread of rabies virus. *Journal of Animal Ecology*, *89*(6), 1375–1386. https://doi.org/10.1111/1365-2656.13176

Palmer, M. W. (1992). The Coexistence of Species in Fractal Landscapes. *The American Naturalist*, *139*(2), 375–397. https://doi.org/10.1086/285332

Pitt, J. A., Larivière, S., & Messier, F. (2008). Survival and Body Condition of Raccoons at the Edge of the Range. *The Journal of Wildlife Management*, *72*(2), 389–395. https://doi.org/10.2193/2005-761

Poisot, T., Borregaard, M. K., Catchen, M. D., Schouten, R., & Baudrot, V. (2023). *NeutralLandscapes* (Version 0.1.3) [Julia]. https://docs.ecojulia.org/NeutralLandscapes.jl/dev/

Prange, S., Gehrt, S. D., & Wiggers, E. P. (2003). Demographic factors contributing to high raccoon densities in urban landscapes. *The Journal of Wildlife Management*, 324–333.

Prange, S., Gehrt, S. D., & Wiggers, E. P. (2004). Influences of anthropogenic resources on raccoon (Procyon lotor) movements and spatial distribution. *Journal of Mammalogy*, *85*(3), 483–490.

Rees, E. E., Pond, B. A., Phillips, J. R., & Murray, D. (2008). Raccoon ecology database: A resource for population dynamics modelling and meta-analysis. *Ecological Informatics*, *3*(1), 87–96. https://doi.org/10.1016/j.ecoinf.2008.01.002

Rees, E. E., Pond, B. A., Tinline, R. R., & Bélanger, D. (2013). Modelling the effect of landscape heterogeneity on the efficacy of vaccination for wildlife infectious disease control. *Journal of Applied Ecology*, *50*(4), 881–891. https://doi.org/10.1111/1365-2664.12101

Sanderson, G. C., & Nalbandov, A. V. (1973). The Reproductive Cycle of the Raccoon in Illinois. *Illinois Natural History Survey Bulletin; v. 031, No. 02*. https://hdl.handle.net/2142/44058

Slate, D., Chipman, R. B., Algeo, T. P., Mills, S. A., Nelson, K. M., Croson, C. K., Dubovi, E. J., Vercauteren, K., Renshaw, R. W., Atwood, T., Johnson, S., & Rupprecht, C. E. (2014). Safety and immunogenicity of Ontario Rabies Vaccine Bait (ONRAB) in the first US field trial in raccoons (Procyon lotor). *Journal of Wildlife Diseases*, *50*(3), 582–595. https://doi.org/10.7589/2013-08-207

Tinline, R., Ball, D., Broadfoot, J., & Pond, B. (2007). The Ontario rabies model. *Queens University, Kingston, Ontario, Canada*.

Tinline, R., Rosatte, R., & MacInnes, C. (2002). Estimating the incubation period of raccoon rabies: A time–space clustering approach. *Preventive Veterinary Medicine, Spatial Epidemiology*, *56*(1), 89–103. https://doi.org/10.1016/S0167-5877(02)00126-5

Appendix 3: Supplemental Tables and Figures

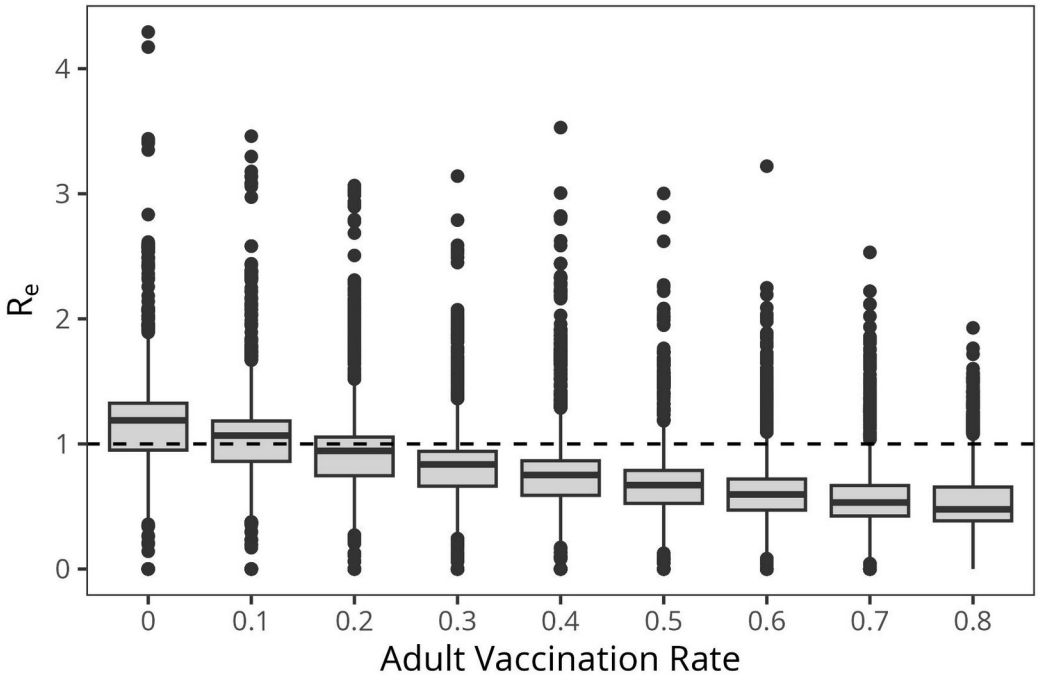

Figure 1. Estimated effective reproduction numbers (R_e) across simulations with varying adult vaccination rates. R_e tended to decrease as the vaccination rate increased, which is expected given the lower proportion of susceptible individuals in the population. Mean estimates of R_e in landscapes with an adult vaccination rate of 0% (1.17) are consistent with empirical estimates (~1.13).

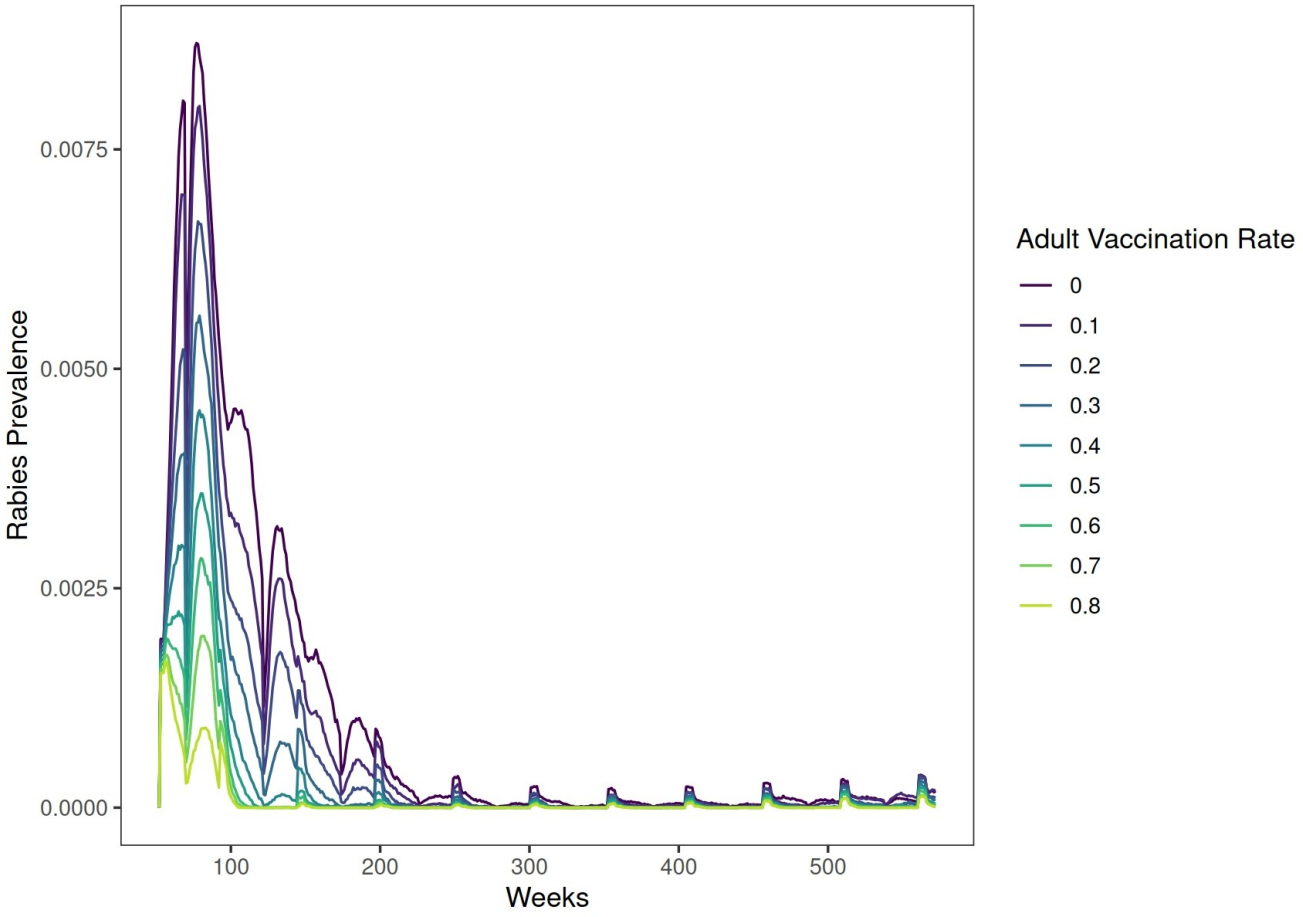

Figure 2. Average weekly rabies prevalence in simulated raccoon populations with varying adult vaccination rates. Prevalence was generally low in all simulations, and was lower in simulations with higher vaccination rates. Increases in average prevalence beyond week 200 correspond to periods of seasonal immigration in some simulations.

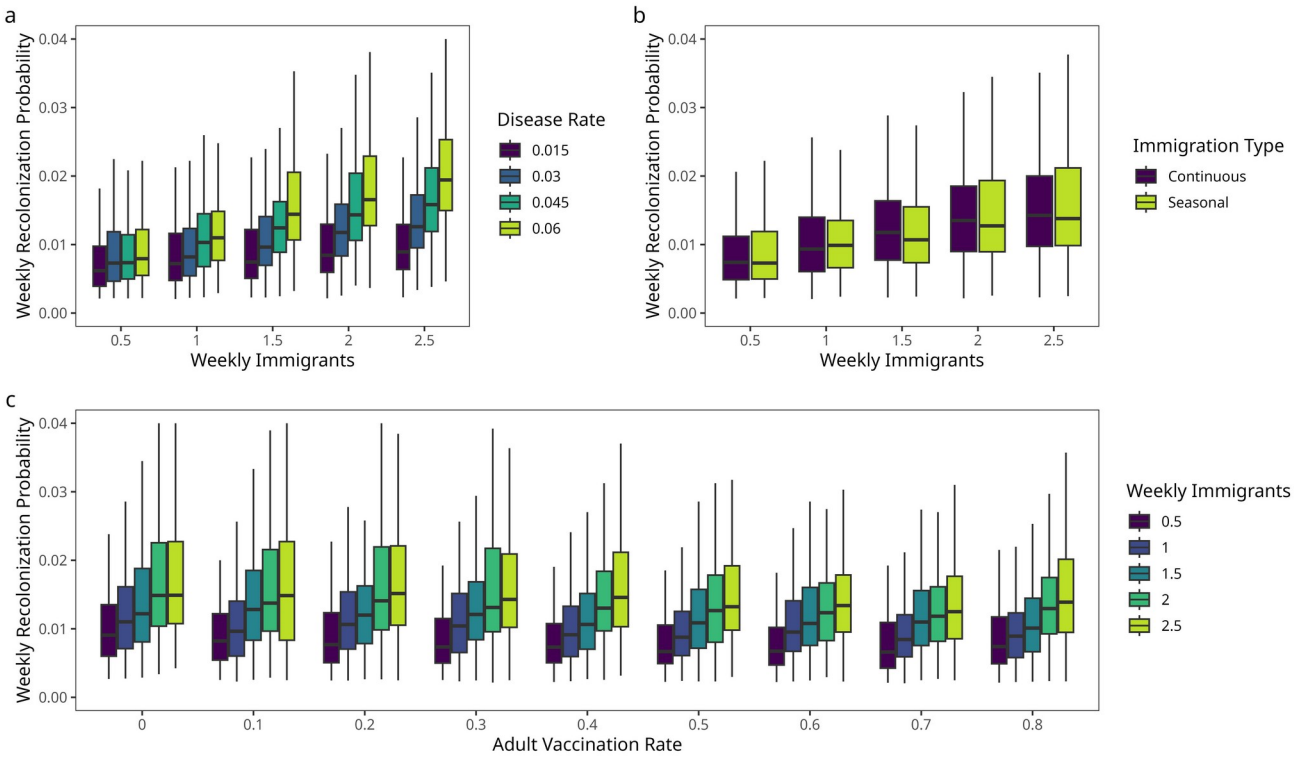

Figure 3. When recolonization was defined as an outbreak occurring after the initial elimination and lasting at least 10 weeks, expected weekly immigrants and immigrant disease rate (i.e. the probability an immigrant was infected with rabies) influenced the weekly probability of rabies recolonization after the initial rabies elimination. Recolonization probability increased by 0.7% with each additional weekly immigrant (a,b), and by with each 1% increase in immigrant disease rate (a). There was no clear effect of immigration type (b) or adult vaccination rate (c) on weekly recolonization probability. Outliers removed for clarity.

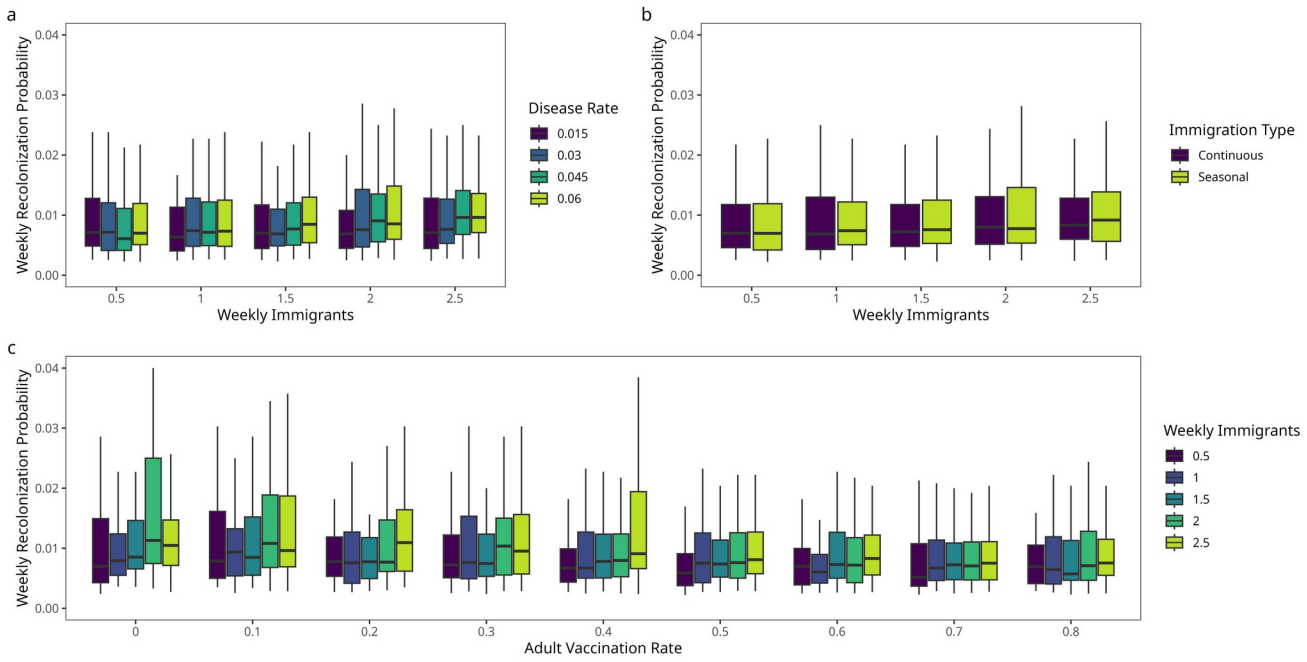

Figure 4. When recolonization was defined as an outbreak occurring after the initial elimination and lasting at least 1 year, there were no clear effects of adult vaccination rates (c) or immigration variables (a–c) on weekly recolonization probability. Outliers removed for clarity.

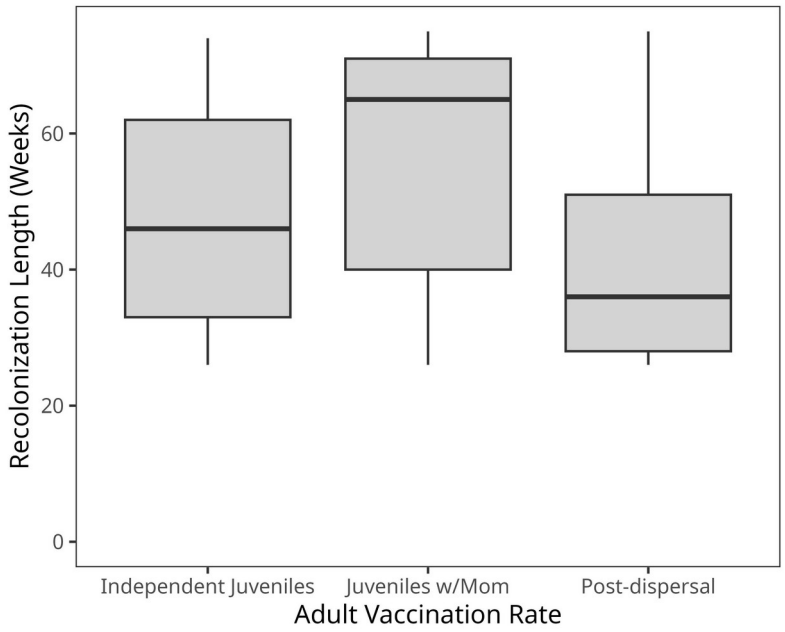

Figure 5. Mean duration of recolonization events, in weeks, based on the timing of the reinfection event. A “recolonization” was defined as a rabies outbreak occurring after the initial elimination and lasting at least 6 months (26 weeks). There were no clear differences in duration between the three time periods.

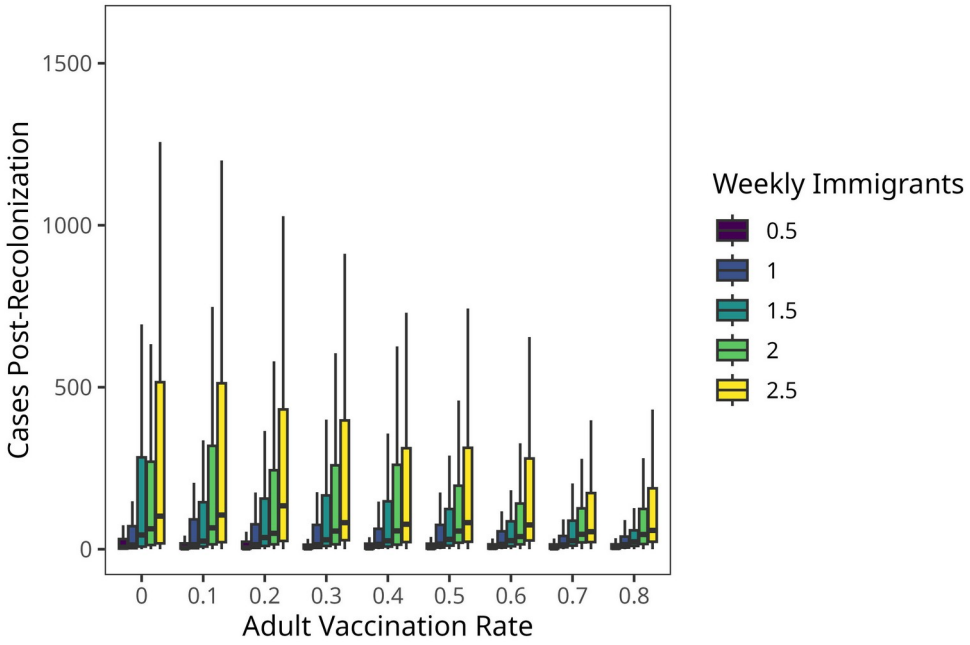

Figure 6. Mean cases after the initial rabies elimination. The number of cases after the initial elimination increased by ~155 cases per increase by 1 weekly immigrant and ~25 cases per 10% increase in adult vaccination rate.